

UNIAXIALLY ALIGNED, POROUS COLLAGEN-GAG SCAFFOLDS FOR *IN VITRO*  
MODELING OF TRABECULAR MESHWORK

by  
Sarah Bernier

A thesis submitted to the Faculty and Board of Trustees of the Colorado School of Mines in partial fulfillment of the requirements for the degree of Master of Science (Chemical Engineering).

Golden, Colorado

Date: \_\_\_\_\_

Signed: \_\_\_\_\_  
Sarah Bernier

Signed: \_\_\_\_\_  
Dr. Melissa Krebs  
Thesis Advisor

Signed: \_\_\_\_\_  
Dr. Mina Pantcheva  
Thesis Advisor

Golden, Colorado

Date: \_\_\_\_\_

Signed: \_\_\_\_\_  
Dr. Colin Wolden  
Professor and Interim Head  
Chemical and Biological Engineering

## ABSTRACT

Glaucoma is the world's leading cause of irreversible blindness. There is currently no cure due to insufficient understanding of the pathology of the disease. Glaucoma has been associated with elevated intraocular pressure. The source of this pressure has been correlated with insufficient outflow of aqueous humor through the trabecular meshwork (TM). The trabecular meshwork is a complex, three dimensional tissue in the eye composed of organized layers of TM cells in an extracellular matrix consisting primarily of collagen and glycosaminoglycan (GAG). Many groups have been studying TM cells *in vitro* to examine their gene expression and response to drugs. However, most *in vitro* studies of TM cells are likely over-simplified since there is a significant difference between the planar surfaces on which the TM cells are traditionally cultured and the complex topographic environment *in vivo*. The physiology of TM cells has been shown to be affected by the topographic cues to which they are exposed. For this reason, there is need for a three dimensional *in vitro* model of the TM for glaucoma drug screening. The goal of this work was to fabricate such a model and explore its interaction with TM cells.

To achieve the overall goal of designing an *in vitro* model, three objectives were outlined: 1) Fabricate collagen-GAG scaffolds with vertically aligned anisotropic pores to mimic the structure of the native tissue. 2) Characterize fabricated scaffolds with scanning electron microscopy (SEM), dynamic mechanical analysis, and glycosaminoglycan quantification. 3) Seed TM cells onto fabricated scaffolds and explore their viability, proliferation, migration, and gene expression.

The first and second goals were achieved in tandem. Uniaxially aligned pores were obtained by employing a unidirectional freezing and lyophilization process. Scanning electron microscopy confirmed the formation of these pores. Image analysis performed on SEM images revealed the average pore diameter to be  $13.7 \pm 5.21 \mu\text{m}$  and the pore density to be 2027 pores/mm<sup>2</sup>. Dynamic mechanical analysis was used to measure the storage modulus of hydrated collagen-only and collagen-GAG scaffolds. There was no statistical difference in the modulus between the two. Glycosaminoglycan content was measured over time using two crosslinking techniques: dehydrothermal crosslinking alone and dehydrothermal crosslinking plus EDC (1-Ethyl-3-(3-dimethylaminopropyl)carbodiimide) chemistry. It was found that both crosslinking techniques resulted in the same rate of elution of GAG from fabricated scaffolds.

The third goal was achieved with various techniques. Viability was tested using fluorescent cellular stains and evaluating cell health over time. A proliferation assay was used to measure growth. Both tests confirmed that cells remained alive and proliferated two weeks after seeding. Histology was used to examine cell proliferation and migration. Histology sections revealed that at lower cell seeding densities, cell preferred to stay near the surface of the scaffolds and remain in contact with each other. At higher seeding densities, there was more migration into the internal pore structure. Gene expression using quantitative polymerase chain reaction (qPCR) was used to confirm the identity of TM cells isolated directly from porcine tissue. The results showed that both isolations of TM cells responded in the expected manner when exposed to glucocorticoids by overexpressing the protein myocilin.

## TABLE OF CONTENTS

|                                                         |      |
|---------------------------------------------------------|------|
| ABSTRACT .....                                          | iii  |
| LIST OF FIGURES.....                                    | viii |
| ACKNOWLEDGEMENTS .....                                  | x    |
| CHAPTER 1 INTRODUCTION AND BACKGROUND .....             | 1    |
| 1.1 Prevalence of Glaucoma .....                        | 1    |
| 1.1.1 Glaucoma Background.....                          | 1    |
| 1.1.2 Current Glaucoma Treatments .....                 | 2    |
| 1.2 Tissue Engineering.....                             | 3    |
| 1.2.1 Collagen Structure.....                           | 4    |
| 1.2.2 The Importance of Crosslinking Collagen.....      | 4    |
| 1.2.3 Cell Selection for Tissue Scaffolds .....         | 5    |
| 1.3 <i>In Vitro</i> Models of Trabecular Meshwork ..... | 6    |
| 1.4 Research Objectives.....                            | 7    |
| 1.4.1 Collagen Scaffold Fabrication.....                | 7    |
| 1.4.2 Characterization of Scaffolds.....                | 8    |
| 1.4.3 TM Cell Culture on Scaffolds.....                 | 9    |
| CHAPTER 2 MATERIALS AND METHODS .....                   | 10   |
| 2.1 Collagen-GAG Scaffold Fabrication.....              | 10   |
| 2.2 SEM Imaging and Pore Size Analysis .....            | 11   |

|                                                                              |    |
|------------------------------------------------------------------------------|----|
| 2.3 Dynamic Mechanical Analysis of Collagen-GAG Scaffolds .....              | 12 |
| 2.4 EDC Crosslinking .....                                                   | 12 |
| 2.5 GAG Quantification .....                                                 | 13 |
| 2.6 Porcine Trabecular Meshwork Cell Isolation and Sub-Culture.....          | 13 |
| 2.7 Culture of Trabecular Meshwork Cells on Collagen-GAG Scaffolds.....      | 14 |
| 2.8 Fluorescent Staining of TM Cells.....                                    | 15 |
| 2.9 Metabolic Assay for TM Cells Seeded on Collagen-GAG Scaffolds .....      | 15 |
| 2.10 Histological Analysis of TM Cells Seeded on Collagen-GAG Scaffolds..... | 16 |
| 2.11 Gene Expression of TM Cells with qPCR .....                             | 16 |
| CHAPTER 3 RESULTS AND DISCUSSION .....                                       | 18 |
| 3.1 Characterization of Collagen-GAG Scaffolds.....                          | 18 |
| 3.1.1 SEM Images of Scaffold Structure.....                                  | 18 |
| 3.1.2 Pore Size Analysis.....                                                | 20 |
| 3.1.3 Dynamic Mechanical Analysis of Collagen-GAG Scaffolds .....            | 21 |
| 3.1.4 Glycosaminoglycan Quantification and Retention .....                   | 24 |
| 3.2 Trabecular Meshwork Cell Viability and Proliferation.....                | 27 |
| 3.2.1 Fluorescent Imaging of TM Cells to Assess Cell Viability .....         | 28 |
| 3.2.2 TM Cell Proliferation .....                                            | 32 |
| 3.3 Histological Analysis of TM Cells on Collagen-GAG Scaffolds.....         | 35 |
| 3.4 Gene Expression of TM Cells.....                                         | 39 |

|                                                            |    |
|------------------------------------------------------------|----|
| CHAPTER 4 SUMMARY AND RECOMMENDATIONS.....                 | 42 |
| 4.1 Summary of Results .....                               | 42 |
| 4.2 Recommendations for Future Work.....                   | 44 |
| 4.2.1 Increasing the Retention of Glycosaminoglycans ..... | 44 |
| 4.2.2 Scaffold Seeding Technique.....                      | 45 |
| 4.2.3 Myocilin Expression of TM Cells on Scaffolds .....   | 46 |
| 4.2.4 Perfusion of Collagen-GAG Scaffolds .....            | 46 |
| 4.3 Conclusion.....                                        | 47 |
| REFERENCES CITED .....                                     | 49 |

## LIST OF FIGURES

|            |                                                                                                                                                                                                                                                                                                                                  |
|------------|----------------------------------------------------------------------------------------------------------------------------------------------------------------------------------------------------------------------------------------------------------------------------------------------------------------------------------|
| Figure 2.1 | Unidirectional freezing is induced when the bottom surface of the copper cap is exposed to liquid nitrogen. A freezing front forms and moves up through the collagen-GAG slurry, displacing the polymer strands. Lyophilization removes the ice crystals and leaves directional pores in the now dry scaffold construct ..... 11 |
| Figure 3.1 | SEM image of the cross section of a 0.3 cm collagen-GAG scaffold. The collagen fibers are visibly aligned from left to right..... 19                                                                                                                                                                                             |
| Figure 3.2 | SEM image of the top surface of a 0.3 cm collagen-GAG scaffold ..... 19                                                                                                                                                                                                                                                          |
| Figure 3.3 | ImageJ analysis of pore size on the surface of a 0.3 cm collagen-GAG scaffold. The threshold tool was used to exploit differences in pixel brightness and select for pores. Areas of noise were excluded ..... 20                                                                                                                |
| Figure 3.4 | Storage modulus of collagen-GAG and collagen-only 0.3 cm hydrated scaffolds. The average is reported at 1% oscillation strain, 1 Hz, and 0.01 N normal force. Measurements were taken at room temperature..... 22                                                                                                                |
| Figure 3.5 | Chondroitin-6-sulfate standard curve. The relationship was linear up to 60 µg/mL. Chondroitin-6-sulfate was dissolved in 0.05 M acetic acid ..... 24                                                                                                                                                                             |
| Figure 3.6 | Glycosaminoglycan content over different time periods using either dehydrothermal crosslinking or dehydrothermal crosslinking plus EDC chemistry. The total GAG refers to the amount of GAG in one digested scaffold. The starting amount used in fabrication was 375 µg per scaffold..... 25                                    |
| Figure 3.7 | 25,000 TM cells seeded on a collagen scaffold and cultured for 2 weeks. Fluorescein diacetate was used to label live cells (in green) and ethidium bromide was used to label dead cells (in blue)..... 29                                                                                                                        |



|             |                                                                                                                                                                                                                                                                  |    |
|-------------|------------------------------------------------------------------------------------------------------------------------------------------------------------------------------------------------------------------------------------------------------------------|----|
| Figure 3.8  | 50,000 TM cells seeded on a collagen scaffold and cultured for 2 weeks. Fluorescein diacetate was used to label live cells (in green). There were no dead cells in this region .....                                                                             | 30 |
| Figure 3.9  | 50,000 cells seeded on a collagen scaffold and cultured for 3 days. CellTracker Green CMFDA used to label live cells.....                                                                                                                                        | 31 |
| Figure 3.10 | 100,000 TM cells seeded on collagen-GAG scaffolds and grown over a 2 week culture period.....                                                                                                                                                                    | 32 |
| Figure 3.11 | 100,000 cells seeded on both scaffolds and in the wells of a 6 well plate. Cells were cultured over a 2 week period and their proliferation measured with an MTS assay .....                                                                                     | 33 |
| Figure 3.12 | 3 $\mu$ m histology section stained with H&E. 100,000 TM cells seeded on a collagen-GAG scaffold and cultured for 2 weeks .....                                                                                                                                  | 36 |
| Figure 3.13 | 3 $\mu$ m histology section stained with H&E. 100,000 TM cells seeded on a collagen-GAG scaffold and cultured for 3 weeks .....                                                                                                                                  | 37 |
| Figure 3.14 | 3 $\mu$ m histology section stained with H&E. 1 million TM cells seeded on a collagen-GAG scaffold and cultured for 1 week .....                                                                                                                                 | 37 |
| Figure 3.15 | 3 $\mu$ m histology section stained with H&E. 1 million TM cells seeded on a collagen-GAG scaffold and cultured for 2 weeks .....                                                                                                                                | 38 |
| Figure 3.16 | Efficiency plot for the qPCR reactions. The $\Delta C_t$ represents the difference in threshold cycle between the target and reference genes ( $C_{t,MYOC} - C_{t,GAPDH}$ ). A cDNA dilution should result in very little change in the $\Delta C_t$ values..... | 41 |
| Figure 3.17 | The fold change in expression of myocilin in TM cells treated with and without dexamethasone. Data are normalized against GAPDH reference genes and a control calibrator .....                                                                                   | 41 |

## ACKNOWLEDGEMENTS

Thank you to Dr. Melissa Krebs and Dr. Mina Pantcheva for advising me throughout this project. Thank you to the members of the Krebs lab for their discussion and advice. Thank you specifically to Mike Riederer for his help obtaining the dynamic mechanical analysis data. Thank you to Dr. David Ammar for his guidance in the isolation and culture of TM cells. Thank you to the Anschutz Medical Campus histologists who processed my histology samples. Lastly, thank you to my parents, Emily, and Michael, for their encouragement throughout this process and willingness to be my personal editors.

# CHAPTER 1

## INTRODUCTION AND BACKGROUND

### **1.1 Prevalence of Glaucoma**

Glaucoma is the world's leading cause of irreversible blindness [1]. In the United States alone, glaucoma affects nearly 4.5 million people. Current National Eye Institute predictions forecast this number to almost double by 2050 [2]. Unfortunately, a cure for glaucoma has not yet been discovered. As a result, there is a large body of research concerning the mechanisms of the disease itself as well as potential therapeutics.

#### **1.1.1 Glaucoma Background**

The mechanisms governing the development of glaucoma are not well understood. Currently, researchers in the field have not been able to conclusively identify a cause and effect relationship. There are, however, risk factors that can contribute to the progression of the disease. The most common form of the disease is known as open-angle glaucoma. To understand open-angle glaucoma, a bit of background on the anatomy of the eye is necessary. The eye produces a fluid called aqueous humor. Aqueous humor is responsible for delivering nutrients to various parts of the eye, as well as carrying away cellular waste products for disposal. As the aqueous humor exits the eye, it must pass through a region called the anterior chamber angle – the area where the iris and the cornea meet. Within this angle is a small region of tissue known as the trabecular meshwork (TM). The TM is composed of

TM cells in a complex, 3-dimensional environment of extracellular matrix (ECM). In certain people, the flow of aqueous humor through the TM becomes hindered. If fluid cannot flow through the TM at a sufficient rate, back pressure can develop. This back pressure is translated into an increase in intraocular pressure, the overall pressure of the internal components of the eye. If left uncontrolled, the elevated intraocular pressure can eventually damage the optic nerve resulting in blindness. Once this has occurred, the damage is irreversible. Intraocular pressure is one of the few modifiable risk factors for glaucoma [2].

### **1.1.2 Current Glaucoma Treatments**

While there is no cure for glaucoma, there are ways to manage the symptoms to prevent irreversible blindness. The most common form of treatment is topical eye drops. These drops help keep intraocular pressure low either by increasing the amount of flow through the TM and an alternative uveoscleral pathway or by decreasing the production of aqueous humor at its source [2]. While they are usually effective, they must be taken for the duration of the patient's life and can cause uncomfortable side effects. When drops can't do enough to lower the pressure, more invasive methods are used. Laser trabeculoplasty uses lasers to treat the TM tissue to increase the flow of fluid while trabeculectomy completely removes a small block of the TM tissue to create a bypass opening [2]. Even with these methods, pressure can still rise to dangerous levels [2]. There is a clear need for a more permanent solution to the problem, and there is a large push in the research community to find a therapeutic that will do the job. Tissue engineering methods can play a beneficial role in aiding this search.

## 1.2 Tissue Engineering

There is great need for replacement tissues [3]. Injury, genetic defects, and disease can cause tissue damage that results in tissues with diminished functionality. While donor transplant can be an effective means of replacement, the need far exceeds the supply. For patients in need of crucial organs, such as hearts and livers, up to 15% of the donor list die each year waiting to receive organs [4]. Furthermore, success of transplantation is not guaranteed due to host rejection. As early as 1933, researchers have been attempting to apply engineering principles to create tissues and tissue scaffolds [4]. The materials used to construct these tissues and scaffolds are crucial to the overall success of the transplant. Much work has been performed to discover biocompatible materials. According to IUPAC recommendations for terminology, biocompatible materials are defined as materials that have the “ability to be in contact with a living system without producing an adverse effect” [5]. Collagen is a promising candidate on this front because it is found in native tissues. Due to its fibrous structure, collagen can be directed into many different forms, allowing a wide range of tissue engineering applications. Collagen has been studied for applications including use in bone and cartilage reconstruction, vascular disease, skin and cornea damage, urogenital systems, and neural systems [6]. Collagen is also useful both *in vivo* and *in vitro*. Its excellent biocompatibility properties allow for transplantation into the body. In addition, it can serve as a useful model system for many applications, including cellular differentiation, cellular interactions, new drug exploration, and more.

### **1.2.1 Collagen Structure**

Collagen's presence in animals is ubiquitous. It is both the most abundant protein overall as well as the most prevalent component of native extracellular matrix (ECM) [7]. Collagen is well known as a fibrous structural protein. Decades of dedicated research have gone towards understanding the structure of collagen and the various forms it takes in the body. The prototypical form of collagen, known as Type I collagen, is now very well understood. Type I collagen is composed of three parallel strands of polypeptides, each coiled into a left handed helix. These strands come together in a right handed helix to form the overall protein structure: a long, fibrous protein [7]. Multiple strands of the protein come together to form a fibril, and multiple fibrils combine to form a collagen fiber [8]. It is this type of collagen that is now widely used as a biomaterial for the fabrication of tissue scaffolds. Generally, Type I collagen is isolated and purified directly from an animal. Bovine collagen from skin and tendons, porcine collagen from skin, and rat collagen from the tail are particularly prevalent in the field [6]. The isolation and purification processes used to obtain the collagen produces a pure, albeit structurally weak product. Untreated scaffolds created from this collagen are typically subject to degradation and deformation from even weak external stresses. It therefore becomes important to modify these scaffolds such that they are structurally resilient while remaining similar to native structures.

### **1.2.2 The Importance of Crosslinking Collagen**

For some tissue scaffold applications, the scaffold must be able to withstand compressive and tensile stresses to mimic the native tissue, such as bone or cartilage

scaffolds. Untreated collagen scaffolds are often not stable enough to fulfill their desired use (they will dissolved in solution), and any structure given to the collagen would most likely be deformed upon the introduction of even small stresses. This is a concern, especially when the given structure is important to cell adhesion, proliferation, and gene and protein expression.

Collagen is native to the body, but small differences in structure between native collagen and implanted collagen can cause an immune response [6]. In some cases, upon implantation the collagen is recognized by native tissues as foreign and degradation processes will quickly destroy untreated scaffolds [8]. For many applications, ultimate degradation is the desired outcome, with healthy native tissues replacing implanted tissues. But if this degradation process happens too quickly the scaffold does not have a chance to reestablish an area of healthy tissue growth. A more controlled rate of degradation is required for a useful construct.

One method of increasing the resilience of these scaffolds is to crosslink the collagen. Crosslinking occurs when polymers are linked by either covalent or ionic bonds. Crosslinking results in a number of benefits. The scaffolds are more resistant to deformation, they are less prone to degradation *in vivo*, and they have lower swelling ratios than their uncrosslinked counter parts [8]. Crosslinking has become standard in the preparation of collagen scaffolds.

### **1.2.3 Cell Selection for Tissue Scaffolds**

The ultimate fate of an engineered collagen scaffold determines whether it is fabricated with or without cells. In certain cases, scaffolds are designed with integrated

biomolecules. These can range from differentiation factors, growth factors, therapeutics, and much more. For some applications, the scaffold is designed to recruit native cells to populate the structure and commence growth, healing, or treatment. In other cases, cells themselves are integrated into the scaffold to mimic native tissue. *In vitro* models rely on the addition of cells to create an environment similar to what would be encountered in the body. *In vitro* models are extremely useful in the study of disease. They can be used to study disease mechanisms and development, as well as test potential therapeutics in a safe, low-risk setting. For glaucoma, *in vitro* models have played an important role in fostering a better understanding of the disease and exploring potential treatments.

### **1.3 *In Vitro* Models of Trabecular Meshwork**

Previous glaucoma research has provided a wealth of knowledge about the trabecular tissue itself and how it is affected in the disease. Imaging has revealed the structure of the TM in detail [9]. The meshwork is composed of three distinct layers of tissue, the corneoscleral (CS) meshwork, uveal (UV) meshwork, and juxtacanalicular connective tissue (JCT). Aqueous humor moves from the CS, through the UV, and out the JCT into a collection channel called the Schlemm's canal [10]. Each layer is primarily composed of interwoven beams of collagen with TM cells dispersed throughout. As fluid moves from the one side of the meshwork to the other, the pores between these beams and cells grow smaller. It is this complex morphology that an ideal *in vitro* model would attempt to capture. The majority of *in vitro* studies have been performed on cells in traditional 2-dimensional cultures. This is advantageous in that



cells can be easily grown, manipulated, and imaged. The complexity of the 3-dimensional environment, however, is completely lost in these types of cultures. Studies have shown that the function of TM cells is affected by their environment, especially with respect to the topographic cues that they receive [11, 12]. Very few attempts have been made to capture this environment, and those that were conducted focused on surface morphology rather than the complete, 3-dimensional environment [11, 13]. In this thesis, a collagen-based tissue scaffold was created to serve as a 3-dimensional *in vitro* model of the trabecular meshwork.

#### **1.4 Research Objectives**

The overall goal of this thesis work was to create a 3-dimensional *in vitro* model of the trabecular meshwork that can ultimately be used for screening potential therapeutics for glaucoma. Towards this end, 3 objectives were outlined: (1) to develop a collagen based tissue scaffold with an internal structure that approximated the native TM tissue. (2) To characterize the scaffolds with respect to porosity and structure, mechanical properties, and GAG content. (3) To examine the growth, proliferation, and gene expression of TM cells seeded on the surface of these scaffolds.

##### **1.4.1 Collagen Scaffold Fabrication**

A key challenge of this project was developing a scaffold with an internal structure that contained vertically aligned, anisotropic pores. In the native tissue, aqueous humor travels from the CS to the Schlemm's canal through pores that have an overall directionality. It was important to preserve this directionality for future studies

that could incorporate fluid flow. Additionally, the function and morphology of the TM cells are directly affected by the environment to which they are exposed. Developing a morphologically similar structure to native tissue was an important step for inducing TM cells to behave as they would in the body. To achieve this goal, a unidirectional freezing and lyophilization process was employed. The resulting scaffolds contained vertically aligned, anisotropic pores of a size comparable to native tissue. **Chapter 2** explains in detail the methods used to fabricate these scaffolds while **Chapter 3** discusses the results of this fabrication.

#### **1.4.2 Characterization of Scaffolds**

The second goal of this thesis work was to characterize fabricated scaffolds in a number of different ways. Scanning electron microscopy (SEM) was used to examine the internal pore structure as well as the surface structure of the scaffolds. Image analysis software was used to determine the average pore size and pore density of fabricated scaffolds. Dynamic mechanical analysis (DMA) was used to determine the storage modulus of fabricated scaffolds. Glycosaminoglycans (GAGs), structural proteins commonly found in ECM, were incorporated to better represent the native tissue. GAGs are responsible for the selectivity of the filtering aspect of TM, as well as help to modulate the resistance to flow through the TM [14]. An assay was used to quantify the amount of GAG at various points of experimentation. The methods for these techniques are presented in **Chapter 2** and the results in **Chapter 3**.

### 1.4.3 TM Cell Culture on Scaffolds

A large portion of this thesis work was dedicated to studying how TM cells interacted with fabricated scaffolds. Cell viability, proliferation, and migration on the scaffolds are crucial components to a functional *in vitro* model. Primary porcine TM cells were isolated and used in all cell experiments. Their identity was ensured using quantitative PCR to measure the expression of a gene with a unique response in TM cells. Assays were used to measure viability and proliferation. Fluorescent imaging and histology were used to visualize cells on scaffolds and assess viability and migration. **Chapter 2** describes the methods used in these experiments and **Chapter 3** presents the results.

## CHAPTER 2

### MATERIALS AND METHODS

#### 2.1 Collagen-GAG Scaffold Fabrication

Unless otherwise noted, all scaffolds were made with the same base solution. A slurry of 0.5% Type I collagen from calf skin and 0.05% chondroitin sulfate from shark cartilage in 0.05 M acetic acid (all Sigma-Aldrich, St. Louis, MO) was mixed according to the methods outlined by Caliarì *et al.* [15]. The slurry was placed on ice to prevent any gelation of the collagen. A homogenizer (Pro Scientific, PRO250 Homogenizer, Oxford, CT) was used at high speed to completely mix the constituents. This took approximately 3-4 minutes. After homogenization, the slurry was briefly placed in a sonication bath to disrupt any bubbles that formed during homogenization. This step is critical to obtaining the final product as bubbles will prevent the formation of aligned pores. Custom freezing molds were made with 2" segments of  $\frac{5}{8}$ " ID flexible PVC tubing and  $\frac{3}{4}$ " copper caps (Home Depot, Atlanta, GA). The bottom of the PVC tubing was wrapped in several layers of Parafilm® (Sigma-Aldrich, St. Louis, MO) to provide a tight seal with the copper caps. For 0.3 cm thick scaffolds, 0.75 mL of the collagen-GAG slurry were delivered to the freezing molds. The bottom surface of the copper was immediately brought into contact with liquid nitrogen. The difference in thermal conductivity between the copper and the PVC resulted in a freezing front that moved up through the slurry. **Figure 2.1** presents a schematic of the unidirectional freezing process. Once completely frozen, scaffolds were lyophilized (FreeZone 4.5 L Benchtop Freeze Dry System, Labconco, Kansas City, MO) for 48 hours to remove the water. Next, to prevent

dissociation in solution, the scaffolds were dehydrothermally crosslinked in a vacuum oven at 105°C for 24 hours. They were stored under vacuum seal in a 4°C refrigerator until further use. To sterilize for cell culture, scaffolds were transferred to 70% ethanol for 24 hours and washed two times in phosphate buffer solution (PBS, Invitrogen, Carlsbad, GA) for 24 hours each. Scaffolds were used within 3 days after sterilization.

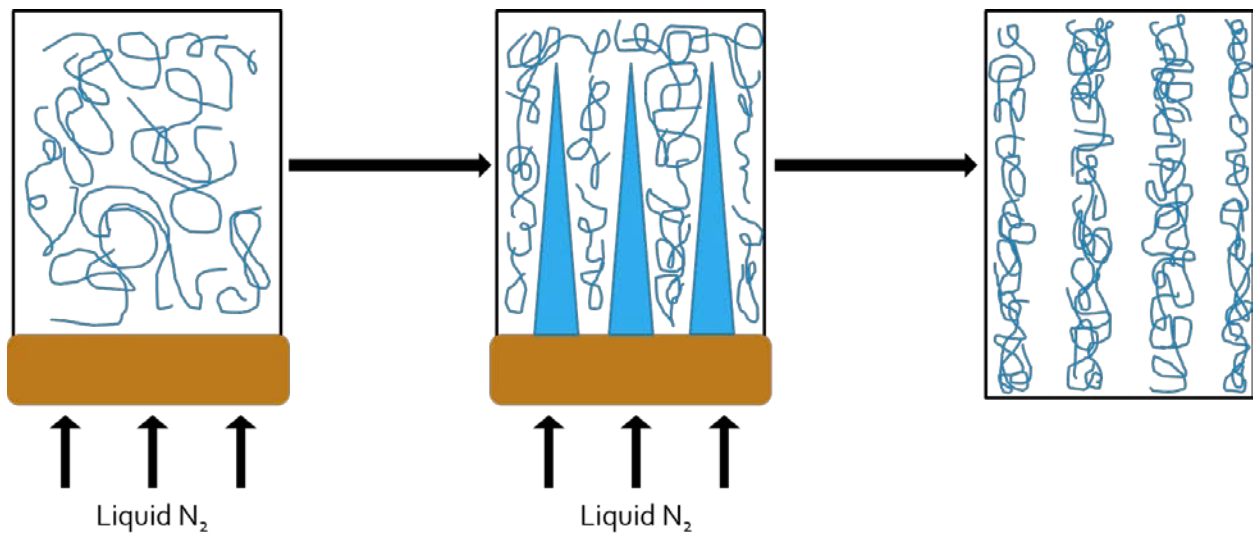


**Figure 2.1** - Unidirectional freezing is induced when the bottom surface of the copper cap is exposed to liquid nitrogen. A freezing front forms and moves up through the collagen-GAG slurry, displacing the polymer strands. Lyophilization removes the ice crystals and leaves directional pores in the now dry scaffold construct.

## 2.2 SEM Imaging and Pore Size Analysis

Scaffold microstructure was examined with an FEI Quanta 600i Environmental Scanning Electron Microscope (Hillsboro, OR) on low vacuum. Samples were prepared by sectioning scaffolds and sputter coating a thin (~5 nm) layer of gold onto the exposed surface. Images were taken 10 mm from the detector with a 20kV accelerating voltage and a spot size ranging from 3.5-5 nm. ImageJ 1.48v (National Institutes of Health,

USA) was used to determine the average pore size and pore density of the scaffolds from the SEM images. The threshold tool was used to exploit differences in pixel brightness and select for pores. A minimum value was set to exclude areas of noise. From this analysis the average pore area and pore density could be determined.

### **2.3 Dynamic Mechanical Analysis of Collagen-GAG Scaffolds**

The storage modulus of both collagen-GAG and collagen only scaffolds was measured using an ARES G2 Rheometer (TA Instruments, New Castle, DE). The collagen-only scaffolds were prepared in exactly the same way as the collagen-GAG scaffolds barring the addition of chondroitin-6-sulfate. Before measurement, scaffolds were hydrated in PBS for approximately 20 minutes. A strain sweep was performed at room temperature and 0.01 N normal force. The frequency was held constant at 1 Hz and the samples were measured using 25 mm parallel plates.

### **2.4 EDC Crosslinking**

To test different crosslinking techniques, some scaffolds were crosslinked using EDC chemistry. The crosslinking solution consisted of 1-Ethyl-3-(3-dimethylaminopropyl)carbodiimide (EDC) and N-hydroxysuccinimide (NHS). A 5:2:1 molar ratio was used for EDAC:NHS:COOH. The carboxylic acid is contributed by the collagen and it is assumed that there are 0.0012 moles COOH per gram collagen. Each scaffold was crosslinked in 1 mL crosslinking solution. Scaffolds were pre-hydrated in half volume PBS (0.5 mL per scaffold) for 15 minutes. The other half volume (0.5 mL) of

PBS containing EDAC and NHS was added to each scaffold and given 30 minutes to crosslink. Scaffolds were then rinsed twice with PBS for 30 minutes each to remove any residual crosslinking solution. Scaffolds were sterilized and used as normal.

## **2.5 GAG Quantification**

Sulfated glycosaminoglycan content was quantified with a dimethylmethylen blue (DMMB) assay. Each scaffold was digested in 3 mL papain buffer (25 µg/mL papain in 50 mM sodium phosphate, 2 mM N-acetyl cysteine, 2 mM EDTA, pH 6.5) overnight at 65°C as described by Ponticiello *et al.* [16]. The digestion process consisted of homogenizing the scaffold in papain buffer for 3-4 minutes until it was completely broken up. After incubation overnight, a DMMB dye solution (21 mg DMMB, 2 g sodium formate, 5 mL absolute ethanol in 1 L distilled water, pH 1.5) was prepared. The digested samples were mixed in a 1:3 ratio with DMMB dye and then further diluted 5x with water to ensure accurate measurement. The absorbance of the resulting solution was measured at 595 nm and compared against a chondroitin sulfate standard curve. The standard curve ranged from 0-60 µg/mL chondroitin-6-sulfate, which covered the linear range of absorbance. All chemicals were purchased from Sigma-Aldrich (St. Louis, MO).

## **2.6 Porcine Trabecular Meshwork Cell Isolation and Sub-Culture**

Porcine eyes were shipped on ice in saline from VisionTech (Mesquite, TX) 24-48 hours post-mortem. The eyes were bisected at the equator and the iris and ciliary

body were removed. The TM region was gently extricated with tweezers and transferred to a dish containing serum free Dulbecco's Modified Eagle's Media (DMEM, Invitrogen, Carlsbad, GA). TM strips were digested in 10 mg/mL collagenase type 4 (Worthington Biochemical, Lakewood, NJ) for 30-60 minutes to dissociate cells. Cells were transferred to a 0.1% gelatin (Sigma-Aldrich, St. Louis, MO) coated 3 cm dish containing DMEM supplemented with fetal bovine serum (10%), penicillin (1%), streptomycin (1%), amphotericin (1:500), and recombinant basic fibroblast growth factor (5 ng/mL) (all Invitrogen, Carlsbad, GA). Once confluent, cells were transferred to a T25 gelatin coated dish using 0.01% trypsin and cultured until confluent. Cells were then transferred to a 10 cm gelatin coated dish and maintained at this size. The culture media was DMEM supplemented with 10% FBS and 1% pen/strep. Culture plates were kept at 37 °C and 5% CO<sub>2</sub>. Cells were used up to passage 8 before they begin to show signs of senescence.

## **2.7 Culture of Trabecular Meshwork Cells on Collagen-GAG Scaffolds**

Sterile scaffolds were prepared by pre-soaking in DMEM (10% FBS, 1% pen/strep) for 30 minutes at 37°C. Pre-soaked scaffolds were transferred to the wells of a non-tissue culture treated 24 well plate. Excess media was aspirated from around the scaffold. Concentrated cell suspensions were prepared and TM cells were delivered onto the surface of each scaffold in ultra-concentrated drops (10-20 µL). Care was taken to ensure that these drops did not overflow the edges of the scaffolds. After cell delivery, scaffolds were incubated at 37°C for 2 hours to promote cell attachment. After



this time period, 1 mL of DMEM (10% FBS, 1% pen/strep) was carefully added to each well. Media was then replaced every 3 days for the duration of each experiment.

## **2.8 Fluorescent Staining of TM Cells**

Two fluorescent stains were used to visualize the viability and location of TM cells seeded on scaffolds. A live/dead stain was prepared by mixing 1 mL fluorescein diacetate (1.5 mg/mL dimethyl sulfoxide (DMSO)), 0.5 mL ethidium bromide (1 mg/mL PBS), and 0.3 mL PBS (all Sigma-Aldrich, St. Louis, MO). To each scaffold containing well, 50  $\mu$ L of this solution were added and given 5 minutes to incubate. Cells were then immediately imaged with a confocal microscope (FV10i-LIV Laser Scanning Microscope, Olympus, Center Valley, PA). CellTracker Green CMFDA (Invitrogen, Carlsbad, GA) was used to label live cells. A 5  $\mu$ M working solution was prepared by first dissolving CellTracker in a very small volume ( $\sim$ 10  $\mu$ L) of DMSO and then diluting to the desired concentration in serum free DMEM. TM cells on 10 cm plates were incubated in dye solution for 30 minutes. Dye solution was then removed and cells were incubated in DMEM with 10% FBS and 1% pen/strep for an additional 30 minutes. CellTracker labeled cells were then seeded onto scaffolds and imaged 1-3 days later using confocal microscopy.

## **2.9 Metabolic Assay for TM Cells Seeded on Collagen-GAG Scaffolds**

Cell viability and proliferation were measured with a standard MTS assay. A 20% CellTiter96 Aqueous One Solution (Promega, Madison, WI) was prepared in PBS.

Scaffolds were incubated in 1 mL CellTiter solution for 100 minutes. The absorbance of the solution was measured at 490 nm in a microplate reader.

## **2.10 Histological Analysis of TM Cells Seeded on Collagen-GAG Scaffolds**

TM cell seeded scaffolds were cultured for 1-3 weeks before fixation in 10% neutral buffered formalin for 24 hours at room temperature. Fixed scaffolds were embedded in paraffin and sectioned into 3  $\mu\text{m}$  slices. Hematoxylin and eosin (H&E) were used to stain the nuclei, cytoplasm, and collagen. Sections were viewed with an Olympus BX41 upright light microscope (Center Valley, PA) and photographed with a Spectra Infinity 1-2CB color camera (Ontario, NY).

## **2.11 Gene Expression of TM Cells with qPCR**

Cellular identity was confirmed using qPCR to measure the expression of the protein myocilin. TM cells were cultured for 5 days with and without 100 nM dexamethasone (Sigma-Aldrich, St. Louis, MO) supplemented media prior to RNA isolation. A High Pure RNA Isolation Kit (Roche Diagnostics, Indianapolis, IN) was used to isolate pure RNA. A Synergy H1 microplate reader (Bio-Tek, Winooski, VT) with a Take3 microplate was used to quantify the RNA concentration and purity after isolation. A Transcriptor First Strand cDNA Synthesis Kit (Roche Diagnostics, Indianapolis, IN) was used to reverse transcribe 1  $\mu\text{g}$  total RNA to cDNA for each sample. Roche's Universal Probe Library was used to design probes and primers for amplifying both myocilin and GAPDH, a common reference gene. Both myocilin and GAPDH genes

were identified for the species *Sus scrofa*. These can be viewed with the accession numbers NM\_213986.1 and NM\_001206359.1 respectively. For the myocilin gene, Universal Probe Library's probe 50 was used. The sequence of this probe is 5'-TCT GGA GC-3'. The left primer used was 5'-CCA TTG TCC TCT CCA AAC TGA-3', and the right primer used was 5'-GGA CTG CTT ACG GAT GTT GG-3'. For the GAPDH gene, Universal Probe Library's probe 28 was used. The sequence of this probe is 5'-CCA GCC GC-3'. The left primer used was 5'-ACA GAC AGC CGT GTG TTC C-3'. The right primer used was 5'-ACC TTC ACC ATC GTG TCT CA-3'. The probes were ordered from Roche. Primers were ordered from Integrated DNA Technologies (Coralville, IA). qPCR was performed on a Roche LightCycler 480 instrument using the Monocolor Hydrolysis Probe/UPL Probe program in 96 Multiwell Plates. The results were analyzed using the  $\Delta\Delta C_t$  method.

## CHAPTER 3

### RESULTS AND DISCUSSION

#### 3.1 Characterization of Collagen-GAG Scaffolds

Various techniques were used to characterize fabricated collagen-GAG scaffolds. This characterization was meant to increase our understanding of the scaffolds as well as provide comparisons with native tissue.

##### 3.1.1 SEM Images of Scaffold Structure

SEM images revealed the internal structure of collagen-GAG scaffolds. **Figure 3.1** is a cross section of a fabricated scaffold. It is positioned such that the top of the scaffold is to the left of the image and the bottom of the scaffold is to the right. **Figure 3.2** is an SEM image of the top surface of a scaffold. Figure 3.1 clearly demonstrates the alignment of the collagen fibers within the scaffold. This is confirmation that the unidirectional freezing technique did induce the formation of aligned pores. It is also seen that the pores are anisotropic. This morphology is similar to the native TM in which interwoven beams of collagen create an organized pore structure that allows for flow of aqueous humor from one side of the meshwork to the other [17]. The pore structure captured by fabricated collagen-GAG scaffolds approximates that structure and provides the topography that may contribute to the proper function of TM cells. The anisotropic nature of the pores is an important source of resistance to flow.

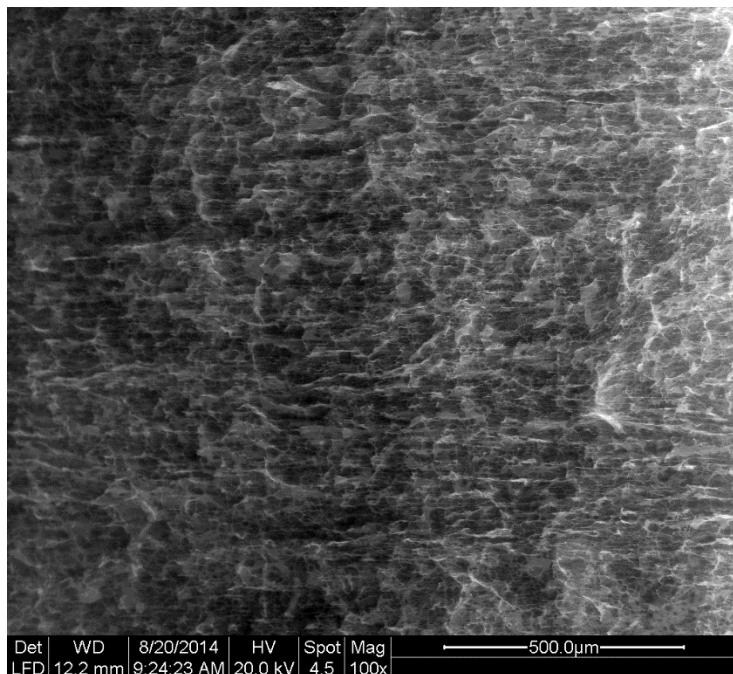


**Figure 3.1** - SEM image of the cross section of a 0.3 cm collagen-GAG scaffold. The collagen fibers are visibly aligned from left to right.

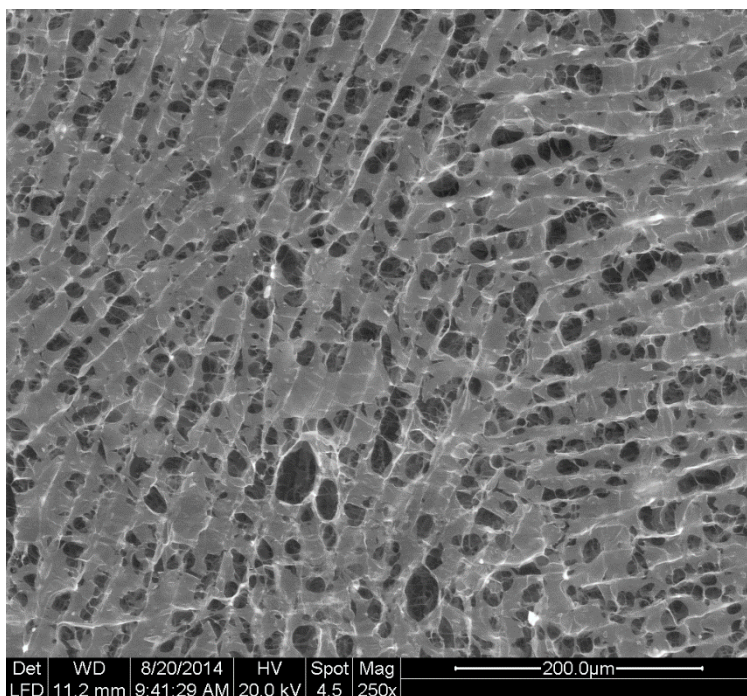


**Figure 3.2** - SEM image of the top surface of a 0.3 cm collagen-GAG scaffold.

Straight, tubular pores, like those used in the *in vitro* model created by Torrejon *et al.*, fail to capture the complexity of native TM and provide very little resistance to fluid flow [13]. Our scaffolds provide a much more realistic environment for TM cells to grow and proliferate. Figure 3.2 confirms that the top surface of fabricated scaffolds contains open pores. Some processing techniques result in a film over the pores that prevents the entrance of cells into the internal structure [18]. Unidirectional freezing results in an open pore structure that allows for the migration of cells into the internal structure.

### 3.1.2 Pore Size Analysis

ImageJ software was used to analyze the average pore size of collagen-GAG scaffolds. **Figure 3.3** shows the result of this analysis.

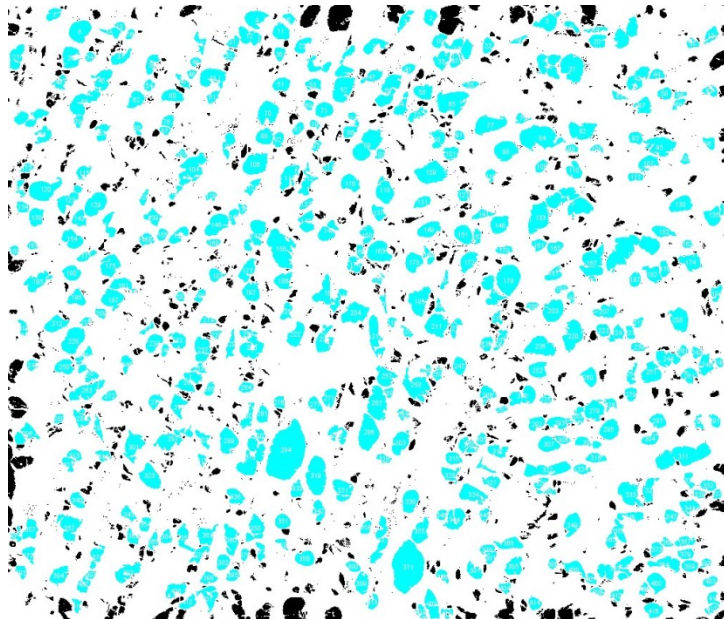


**Figure 3.3** - ImageJ analysis of pore size on the surface of a 0.3 cm collagen-GAG scaffold. The threshold tool was used to exploit differences in pixel brightness and select for pores. Areas of noise were excluded.

The areas in blue represent the pores that have been accounted for in the calculations. The areas in black were considered noise and not actual pores, so they were excluded from the calculation. ImageJ calculated the area of each pore in the image. An assumption was made that each pore could be approximated as a circle. The average pore diameter was found to be  $13.7 \pm 5.21 \mu\text{m}$ . The pore density was also collected from this analysis and found to be 2027 pores/ $\text{mm}^2$ . These results provide a method for comparing our scaffold with native TM. Allingham *et al.* found that the average pore density for normal TM was  $1437 \pm 423 \text{ pores}/\text{mm}^2$  [19]. This is on the same order of magnitude as the pore density obtained in fabricated scaffolds. It has previously been reported that the pore size of trabecular meshwork varies from 4-7  $\mu\text{m}$  in the juxtacanalicular tissue, up to 30  $\mu\text{m}$  in the corneoscleral meshwork, and up to 70  $\mu\text{m}$  in the uveal meshwork [20]. The uveal meshwork is thought to provide little to no resistance to outflow of aqueous humor [21], so the pore size range of the juxtacanalicular and corneoscleral sections are better targets for pore size. Additionally, pores that are too large lead to decreased attachment and proliferation as evidenced by Torrejon *et al.* who found that TM cells responded with the best growth and attachment to 12  $\mu\text{m}$  pores, which matches up very well with the average pore size attained in fabricated scaffolds [13].

### **3.1.3 Dynamic Mechanical Analysis of Collagen-GAG Scaffolds**

Fabricated collagen-GAG scaffolds were tested with dynamic mechanical analysis to determine the average storage modulus. They were compared with

collagen-only scaffolds. The results of this analysis are presented in **Figure 3.4**. The modulus is reported at 1% oscillation strain, 1 Hz, and 0.01 N normal force.

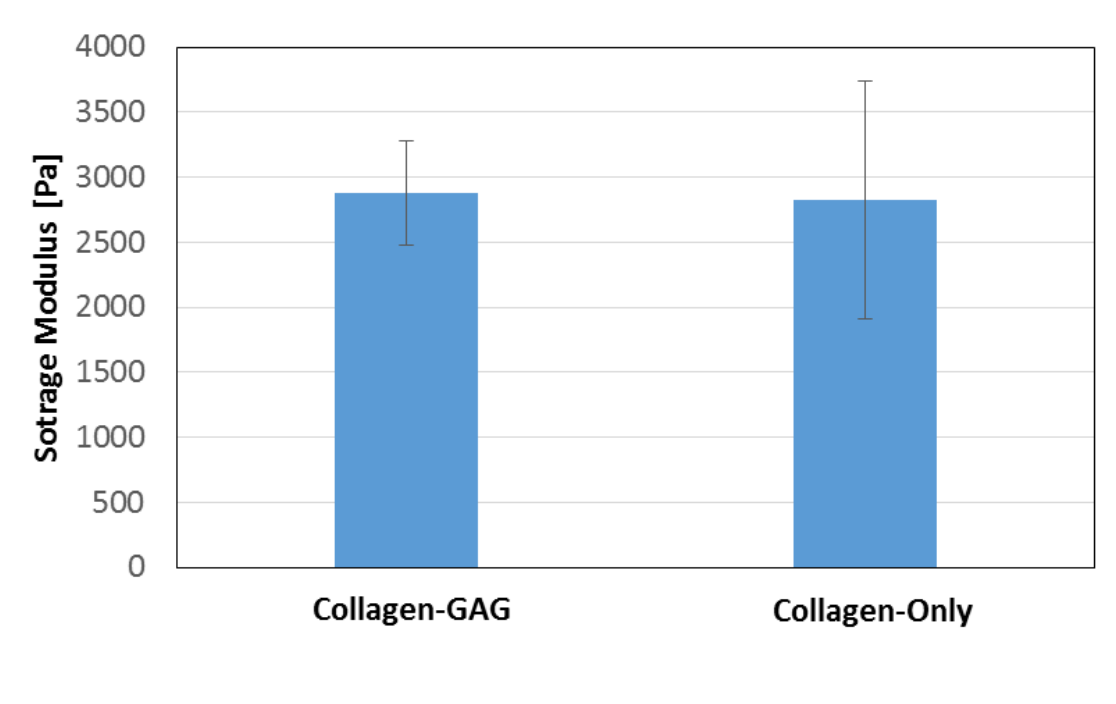


**Figure 3.4** - Storage modulus of collagen-GAG and collagen-only 0.3 cm hydrated scaffolds. The average is reported at 1% oscillation strain, 1 Hz, and 0.01 N normal force. Measurements were taken at room temperature.

The storage modulus of collagen-GAG and collagen-only scaffolds was found to be statistically the same. It was initially predicted that the collagen-GAG scaffolds would have a higher storage modulus owing to the effect of the glycosaminoglycan content. However, the results would indicate that the proportion of GAG present in scaffolds is not sufficient to play a role in the storage modulus. The addition of GAG to scaffolds was not primarily intended to strengthen them, but rather to better mimic the constituents of native tissue in which GAG contributes to the filtering action of the TM as well as helps to modulate resistance to outflow of aqueous humor [14].



The storage modulus obtained through experimentation can be indirectly compared to mechanical measurements that have been obtained for native TM tissue. To date, TM has not been tested using DMA so there is no way to directly compare our results with native tissue. However, correlations with literature can provide some idea of the stiffness of TM tissue compared to fabricated scaffolds. It has been shown that glaucomatous TM is stiffer than normal TM [21-23]. The relationship between stiffness and outflow facility is less clear. While Russel *et al.* showed that outflow facility decreased with increasing stiffness [21], Camras *et al.* found conflicting evidence that increased stiffness actually increased the outflow facility [22]. The difference is thought to be due to the measurement techniques. Russel *et al.* used atomic force microscopy to measure the elastic modulus. This results in a local measurement that can vary over the entire tissue. Camras *et al.* found the apparent bulk elastic modulus of TM using tensile testing. Their results differ significantly, with Russel *et al.* reporting an elastic modulus in normal TM of  $4.0 \pm 2.2$  kPa and Camras *et al.* reporting an elastic modulus in normal TM of  $515 \pm 136$  kPa. These measurements indicate that the stiffness can vary based on the scale that it is being examined (i.e. cellular or bulk). Elastic modulus and storage modulus are not exactly the same measurement and therefore cannot be directly compared, however, they both allude to the stiffness of a material. The storage modulus of fabricated collagen-GAG scaffolds was found to be  $2.9 \pm 0.4$  kPa. While this matches well with Russel *et al.*, it is much lower than the modulus found by Camras *et al.* Future tests with perfusion will determine whether or not amendments to scaffold processing should be made to increase the stiffness of fabricated scaffolds. This could be done in several ways, including increasing the weight percent of collagen, increasing

the weight percent of GAG, or increasing the degree of crosslinking by incorporating additional chemical methods.

### 3.1.4 Glycosaminoglycan Quantification and Retention

Glycosaminoglycans are unbranched polysaccharides that play dual roles in trabecular meshwork. They affect both the structure and the physiologic function of the tissue. In this work, a DMMB assay was used to quantify the amount of GAG incorporated into fabricated scaffolds and explore its retention over the course of several weeks in solution. **Figure 3.5** shows the standard curve used for quantification. It contains chondroitin-6-sulfate from 0-60  $\mu\text{g}/\text{mL}$  in 0.05 M acetic acid.

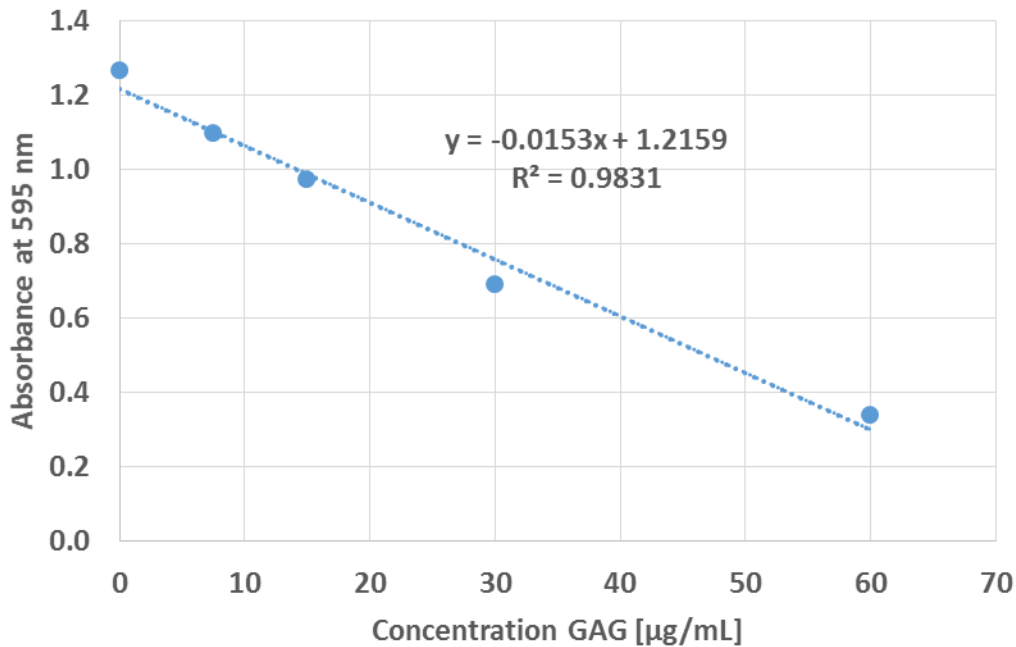


**Figure 3.5** - Chondroitin-6-sulfate standard curve. The relationship was linear up to 60  $\mu\text{g}/\text{mL}$ . Chondroitin-6-sulfate was dissolved in 0.05 M acetic acid.

**Figure 3.6** presents a comparison in retention over the course of two weeks using two different crosslinking techniques, dehydrothermal crosslinking and dehydrothermal crosslinking plus the addition of crosslinking with EDC chemistry.

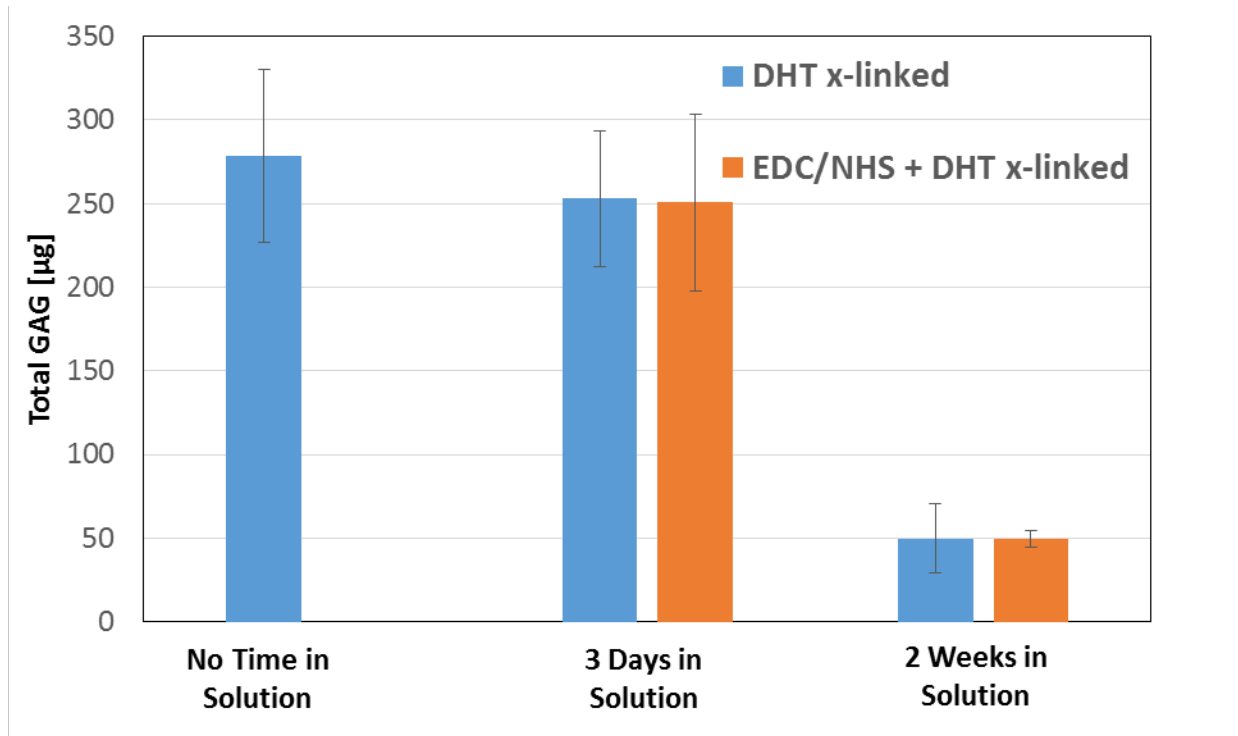


**Figure 3.6** - Glycosaminoglycan content over different time periods using either dehydrothermal crosslinking or dehydrothermal crosslinking plus EDC chemistry. The total GAG refers to the amount of GAG in one digested scaffold. The starting amount used in fabrication was 375 µg per scaffold.

The results show that GAG was rapidly eluted from fabricated scaffolds over the course of two weeks. There was no difference in retention between the two crosslinking methods. This was an unexpected result considering the mechanism involved in each crosslinking method. Dehydrothermal crosslinking of collagen is achieved through exposure to heat under a vacuum. Typically, a lyophilized scaffold is placed in a

vacuum oven for a period ranging from one to several days in temperatures ranging from 100-180°C [24]. The heat induces covalent bonds through condensation reactions between the carboxyl and amino groups that become exposed during crosslinking [25]. This is a purely physical method because there are no chemicals added to induce bonds. The bonds prevent the long collagen molecules from sliding along each other, which increases the stiffness of the scaffold and prevents it from dissolving in solution. EDC chemistry works by activating carboxyl groups to form covalent bonds with primary amine groups. This reaction is facilitated by the addition of *N*-hydroxysuccinimide. In theory, both methods should result in some crosslinking between collagen and GAG. Previous work has shown that using dehydrothermal crosslinking followed by EDC chemistry results in better retention of GAG rather than using dehydrothermal crosslinking alone [26]. Our results, however, show that GAGs are eluted at the same rate regardless of the crosslinking method. A closer look at the chemistry involved seems to explain this phenomenon. Collagen and glycosaminoglycan will only co-precipitate in acidic pH. This is why 0.05 M acetic acid is used as the base solution in the collagen-GAG slurry. It has been shown that the lower the pH, the higher the degree of co-precipitation, up to a limit at which point no more GAG can be added [27]. The acidity of the environment allows for ionic interactions between the collagen and the GAG. These interactions keep the GAG in the construct through the freezing and lyophilization process. Dehydrothermal crosslinking is then used to crosslink collagen to collagen as well as collagen to GAG. The heating process exposes residues on the collagen that would otherwise be inaccessible due to its tightly wound helical structure. These exposed residues covalently link the collagen to itself as well as a proportion of

the available GAG. There are only so many available binding sites exposed during this process and it is thought that they saturate [27]. This would explain why there was no difference in retention when EDC chemistry was used in addition to dehydrothermal crosslinking. With all of the available binding sites already taken, the EDC is not able to activate carboxyl groups and create additional bonds. This would also explain why the GAG elutes when placed in solution. While some of the GAG is covalently linked to collagen, the majority is only held by ionic interaction or physical entrapment. When placed in neutral solution, such as PBS or cell media, the ionic interactions disband and the GAG is free to diffuse into solution.

The problem of GAG retention is not unique to this work [28, 29]. Tissue engineering constructs have long suffered from low retention rates. There are some techniques that have slowed the rate of retention, such as amination of collagen, but ultimately the GAG still elutes over time. For our purpose, GAG is incorporated to expose the TM cells to components that they would see in the native tissue. Yue *et al.* showed that the physiology of TM cells is affected by GAG content [30]. While the GAG does elute into solution, the TM cells are still exposed to the GAGs over time and continue to secrete their own GAGs [28]. For this reason, the elution of GAG is not considered an insurmountable problem toward developing this *in vitro* model.

### **3.2 Trabecular Meshwork Cell Viability and Proliferation**

TM cells seeded on collagen-GAG scaffolds are expected to maintain viability and proliferate for a period of time that allows for useful *in vitro* testing of therapeutics.

Most therapeutics are efficacious on the time scale of hours [31]. A useful *in vitro* model should allow for testing over the course of several days with these types of therapeutics to observe the effect of multiple doses. To test the viability and proliferation of fabricated scaffolds, fluorescent cellular stains and a metabolic assay were used.

### 3.2.1 Fluorescent Imaging of TM Cells to Assess Cell Viability

Fluorescein diacetate and ethidium bromide are a combination live/dead stain used to measure viability at a single point in time. Fluorescein diacetate is only active when exposed to the enzymatic activity of live cells and can only permeate the cell membranes of live cells [32]. Ethidium bromide labels the DNA of dead cells whose cellular membranes have broken down. **Figure 3.7** shows both live and dead labeled cells, ensuring that both labels are working properly. Higher seeding densities were tested with the live/dead stain to explore viability and location on the scaffolds. **Figure 3.8** shows results from this higher seeding experiment. The higher seeding density seems to result in cells that express a healthier morphology. In both native tissue and 2D culture, TM cells tend to produce lots of extracellular matrix (ECM) [13]. TM cells benefit from cell-cell contact with one another and prefer to be close to their counterparts [17]. In **Figure 3.7**, even after two weeks in culture, the cells remained in a balled up morphology. There were also a few dead cells interspersed with the live cells. **Figure 3.8** presents very different cell morphology. Here, the cells have taken on a more elongated form like their native counterparts. These early viability experiments led us to increase our seeding densities throughout future experiments. Ultimately, problems were encountered with the collagen itself incorporating the fluorescein diacetate and

fluorescing. This made it very difficult to find areas on the scaffolds where the cells could be distinguished from the fluorescent collagen. A different type of fluorescent dye was used to try to mitigate this issue.

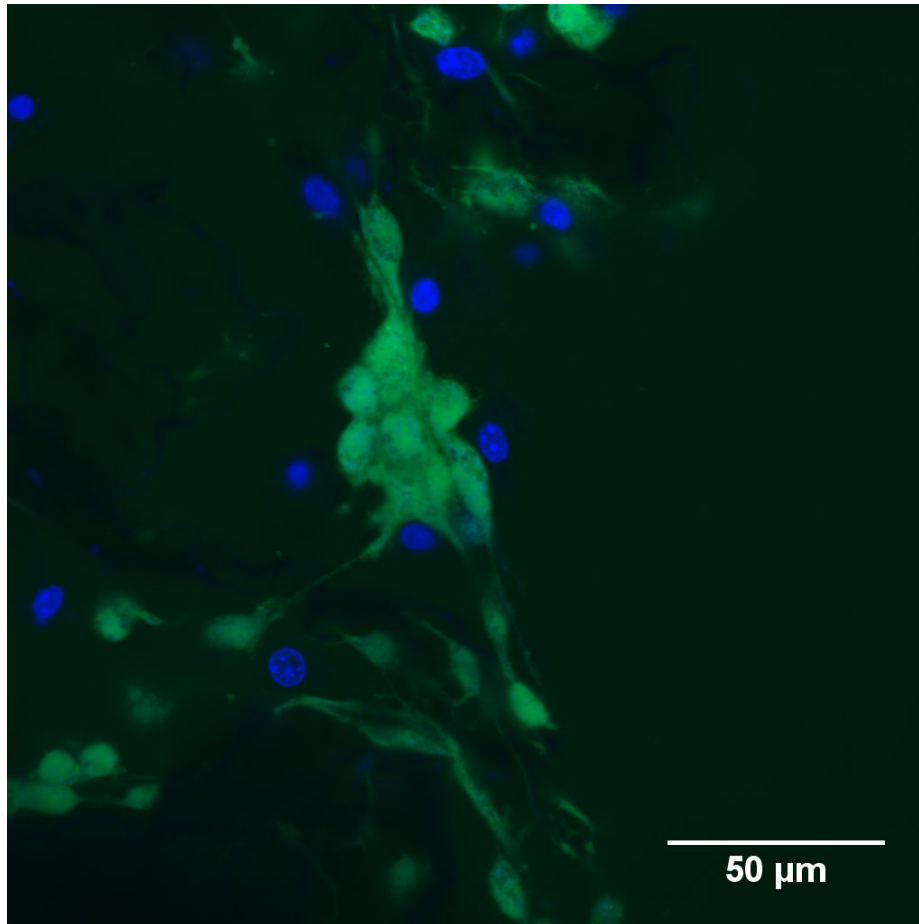


**Figure 3.7** - 25,000 TM cells seeded on a collagen scaffold and cultured for 2 weeks. Fluorescein diacetate was used to label live cells (in green) and ethidium bromide was used to label dead cells (in blue).

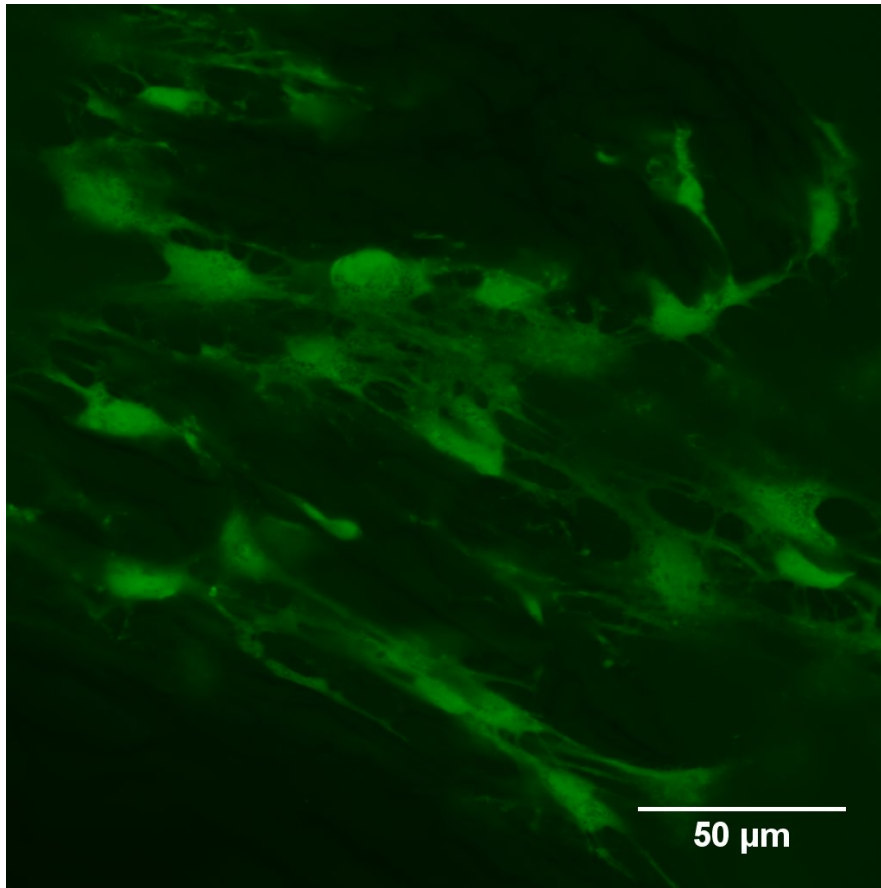


**Figure 3.8** - 50,000 TM cells seeded on a collagen scaffold and cultured for 2 weeks. Fluorescein diacetate was used to label live cells (in green). There were no dead cells in this region.

CellTracker Green CMFDA is a cellular dye that can freely pass through cellular membranes, but once inside a live cell, it undergoes a chemical reaction that converts it to an impermeable fluorescent product [33]. It is advantageous in that unlike a live/dead stain, which is sacrificial, CellTracker dyes can be imaged for several days and are passed onto daughter cells, but not neighbors. By staining cells before seeding onto scaffolds, the issue of the collagen picking up the stain and fluorescing was avoided.

**Figure 3.9** shows a representative image of CellTracker Green labeled cells on a



fabricated scaffold. High numbers of live cells were seen on the surface indicating good cell viability.

Fluorescent imaging was a good starting point for assessing cell viability, but ultimately could only be used to see surface cells. Collagen's opaque nature prevented the confocal microscopy from capturing detail below the scaffold surface. For this reason, several other techniques were employed to assess TM cells seeded on collagen-GAG scaffolds.

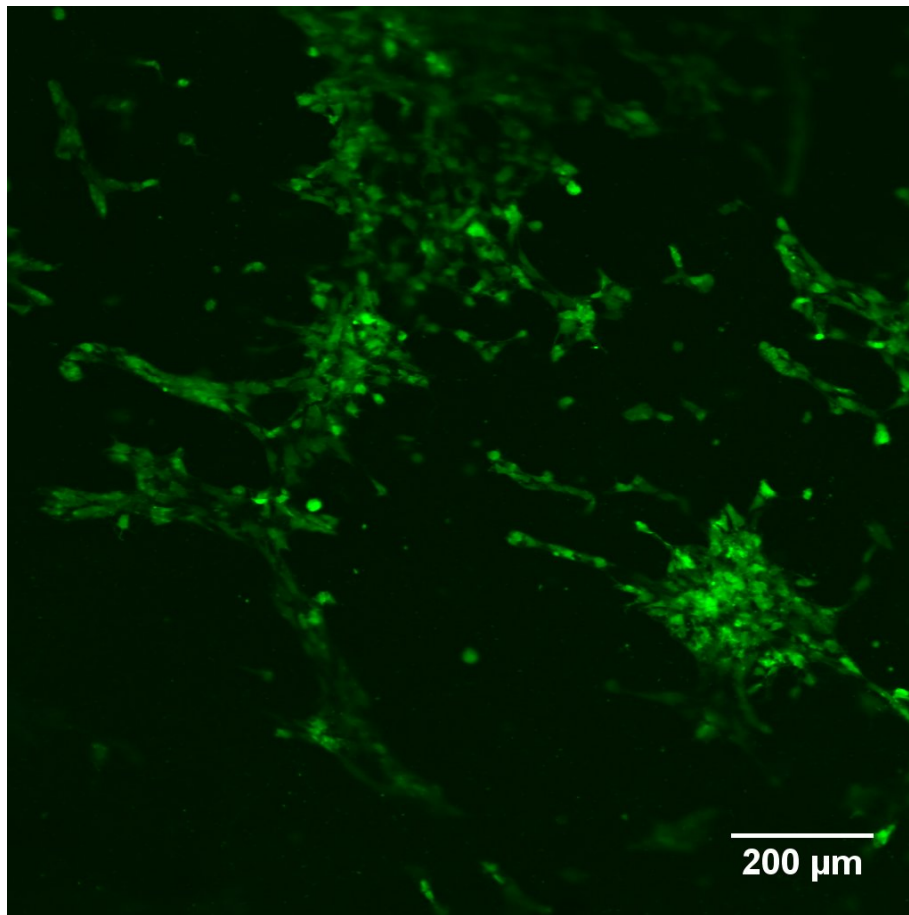


**Figure 3.9** - 50,000 cells seeded on a collagen scaffold and cultured for 3 days. CellTracker Green CMFDA used to label live cells.

### 3.2.2 TM Cell Proliferation

An MTS assay was used to measure proliferation of TM cells seeded on collagen-GAG scaffolds over several weeks in culture. MTS is a chemical that undergoes a reaction with metabolic products created by cells to produce formazan, a colored chemical that can be identified with absorbance measurements [34]. The more metabolic product present (indicating more cells overall), the more formazan produced and the higher the absorbance reading. **Figure 3.10** presents the results of a 2-week experiment.

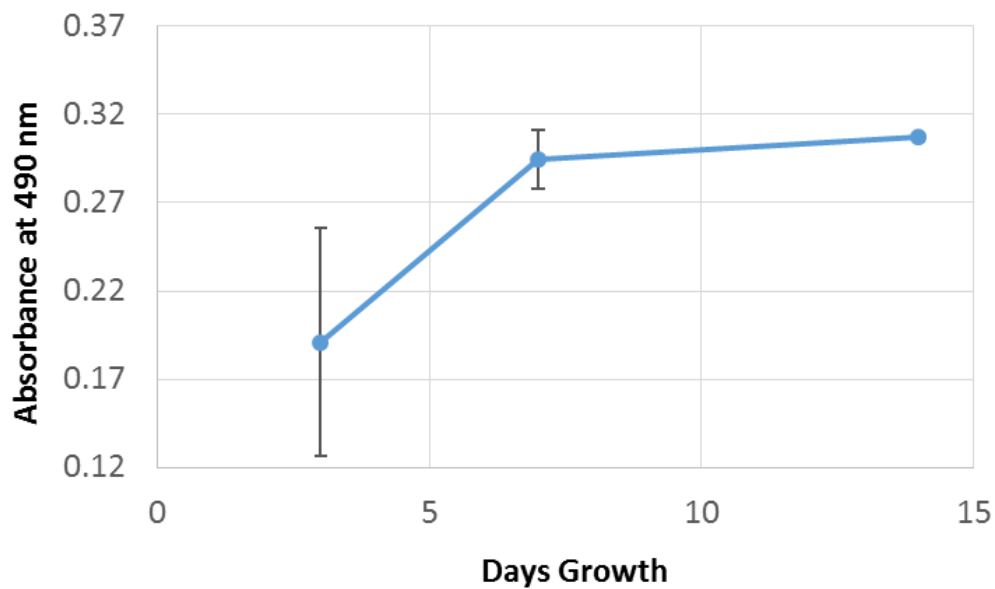


**Figure 3.10** - 100,000 TM cells seeded on collagen-GAG scaffolds and grown over a 2 week culture period.

From day 3 to week 1, there was a 60% increase in proliferation. From week 1 to week 2, this dropped to a 5% increase. The reason for this slowed proliferation is not clear. It is possible that the cells are not as metabolically active as the culture period is

increased, which would lead to a decrease in absorbance. It is also possible that the cells simply stop proliferating, indicating that something in their environment has affected their growth. The same initial number of cells (100,000) cultured in a 6 well plate over the same time period served as a comparison for cells on scaffolds. **Figure 3.11** presents these comparative data on the same plot. The results from the 6 well plate indicate that there were slightly more cells throughout the 2 week culture period. This is to be expected, as there is almost certainly some cell death during scaffold seeding due to either spillover of the concentrated cell suspension or weak attachment of some cells to the surface.

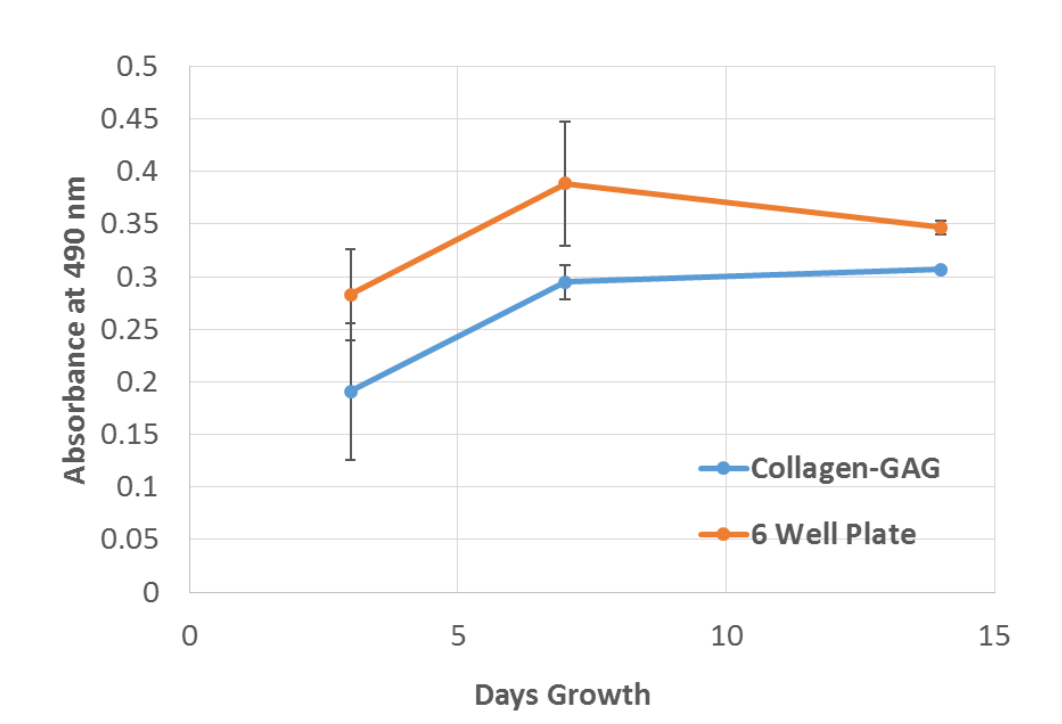


**Figure 3.11** - 100,000 cells seeded on both scaffolds and in the wells of a 6 well plate. Cells were cultured over a 2 week period and their proliferation measured with an MTS assay.

Like the collagen-GAG scaffolds, from day 3 to week 1, proliferation increases at an almost identical rate. However, between 1 and 2 weeks in culture, proliferation began to decline. In 2D cell culture, there is a finite amount of space that can be occupied by cells. Once they become confluent on the plate, they essentially run out of room to grow and their viability can go down if they aren't passaged onto a new surface. This would explain the decrease seen between weeks 1 and 2 in the 6 well plate experiment. On scaffolds, there is much more surface area available for growth. The expectation would be for the cells to continue to proliferate at a steady pace as they migrate to new areas of the scaffold. While they are still proliferating at 2 weeks, their proliferation slows substantially. The most likely reason for this decrease is that there is actually too much surface area for the number of cells seeded. When the cells are first delivered to the scaffold, it is in a concentrated drop of cell suspension. For the first week in culture, they are near each other and proliferate like they would on a plate. As they begin to spread out and migrate to other parts of the scaffold, they become less and less dense. As mentioned previously, TM cells are more viable when in contact with one another [17]. The evidence suggests that as they spread further, they become less robust and their growth slows. Future work will repeat this experiment with higher cell densities to test this hypothesis. Despite the slowed proliferation, this experiment demonstrated that cells seeded on scaffolds remain viable and continue to grow 2 weeks after seeding. This is enough time to test the short-term efficacy of current and potential glaucoma therapeutics.

### 3.3 Histological Analysis of TM Cells on Collagen-GAG Scaffolds

Histology is a widely used technique for tissue examination in both research and clinical settings. Physicians use histology as a diagnostic tool to determine whether specific disease markers are present in tissue samples. Histology can make use of immunohistochemistry, the chemistry of antigen-antibody interactions [35]. Tissue samples are fixed, dehydrated, and embedded in paraffin wax. The resulting tissue blocks can then be sliced into sections as thin as 3  $\mu\text{m}$ . These sections are stained with antibodies that are specific for certain biomarkers. For this work, histology was used to label the collagen, cell nuclei, and cell cytoplasm. The goal was to visualize both how many cells were visible as well as where they had migrated during specific time periods in culture. **Figure 3.12** is a histology section showing TM cells on a collagen-GAG scaffold. TM cells formed a layer on the surface of the scaffold and several cells migrated further into the internal structure. Compared to the scaffolds processed at 1 week in culture, there were more cells in the internal of the scaffold at 2 weeks, indicating that migration was actively occurring. Between 2 and 3 weeks, however, there was not a noticeable difference in cell migration. This result correlates well with the results of the MTS assay. After two weeks in culture, proliferation began to slow. It was hypothesized that this was due to the lack of cell-cell contact between TM cells. From the histology images, the cells that migrate into the internal structure are typically isolated from their neighbors. This isolation could contribute to the lack of further migration or proliferation between weeks 2 and 3. Certain sections of the scaffolds contained very little migration. This was further indication that the cells prefer to stay

close to their counterparts instead of migrating to less dense areas of the scaffolds.

**Figure 3.13** is an example of this type of morphology.

In general, the areas that had more migration inward did not have cells in multilayer on the surface, and vice versa. Another experiment was performed that increased the cell seeding to 1 million cells per scaffold. The idea was that the higher seeding density would encourage more cells to migrate inward to take advantage of the increased surface area available. **Figure 3.14** shows the results after 1 week in culture.

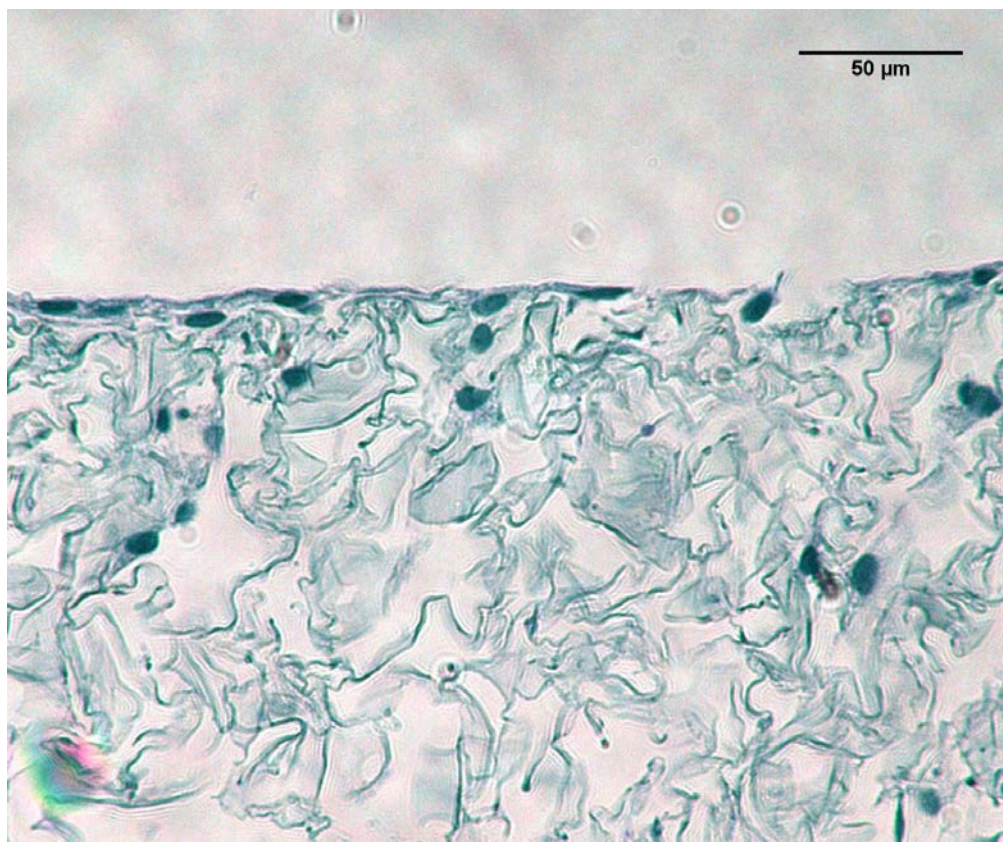


**Figure 3.12** - 3 μm histology section stained with H&E. 100,000 TM cells seeded on a collagen-GAG scaffold and cultured for 2 weeks.



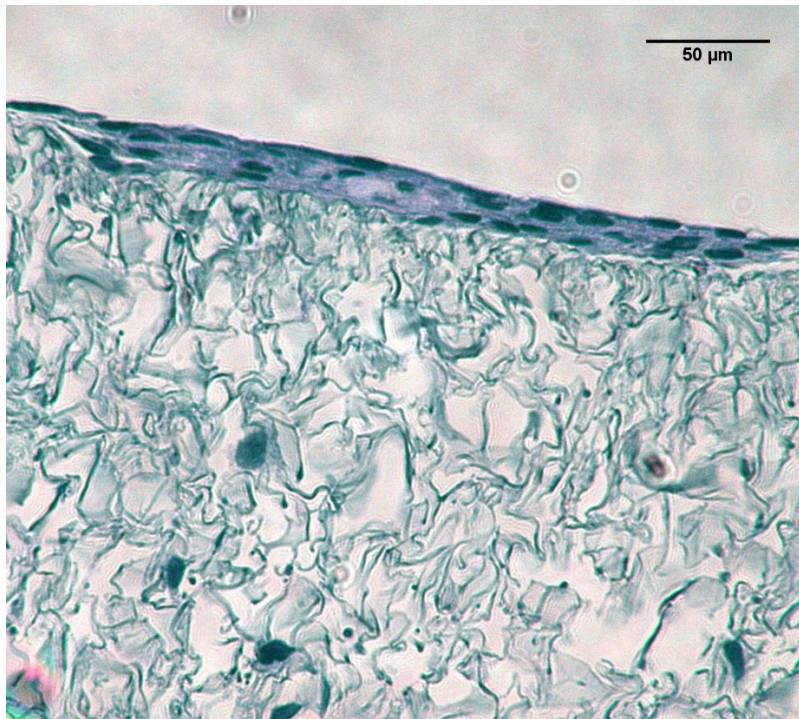


**Figure 3.13** - 3 μm histology section stained with H&E. 100,000 TM cells seeded on a collagen-GAG scaffold and cultured for 3 weeks.

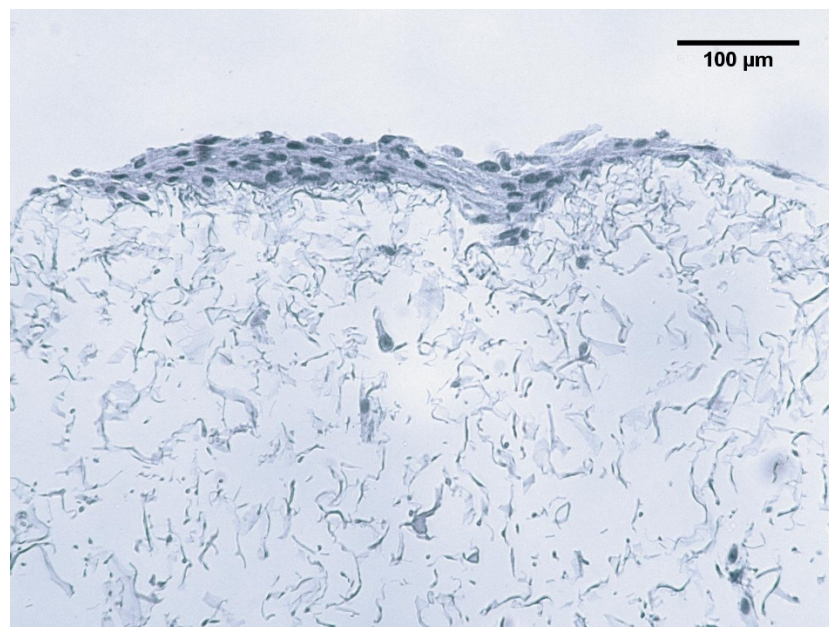


**Figure 3.14** - 3 μm histology section stained with H&E. 1 million TM cells seeded on a collagen-GAG scaffold and cultured for 1 week.

Again, there were regions of high cell densities on the surface, and regions of more migration into the internal structure. However, cell numbers overall were increased from the scaffolds seeded with 100,000 cells. **Figure 3.15** shows a region which had migration far into the internal structure.



**Figure 3.15** - 3  $\mu\text{m}$  histology section stained with H&E. 1 million TM cells seeded on a collagen-GAG scaffold and cultured for 2 weeks.

TM cells penetrated several hundred microns into the internal structure of the scaffold. This was much further than anything seen in the scaffolds seeded with 100,000 cells. This would indicate that higher seeding numbers result in more migration and penetration into the internal structure.



Previous studies have found similar results when working with fabricated tissue constructs. Thevenot *et al.* tested the penetration and distribution of cells seeded onto porous, poly(lactide-co-glycolide) (PLGA) based scaffolds using various seeding techniques [36]. Static seeding, the technique used in this work, involves delivering a concentrated cell suspension directly to the surface of the scaffold. Thevenot found that static seeding resulted in the majority of the cells occupying the surface of the scaffold with very little penetration past a depth of 900  $\mu\text{m}$ . Static seeding is traditionally used because it is fast, convenient, and results in high cell viability [37, 38]. Recently, dynamic seeding techniques have been shown to result in better cell penetration and distribution in 3D tissue constructs [39-41]. Thevenot *et al.*'s work showed that orbital seeding, agitating the construct in media containing unattached cells, resulted in the most even distribution of cells within the construct. This technique was not used in this work, but could be a good option for future work.

### **3.4 Gene Expression of TM Cells**

Characterization of gene expression is a powerful tool for understanding the function of cells at a much deeper level. The trabecular meshwork cells are unique in that they have a gene with an inducible glucocorticoid response [42]. This gene, MYOC, expresses the protein myocilin in higher amounts when the TM tissue is exposed to glucocorticoids, such as dexamethasone [43]. This response is useful for a variety of reasons. It can be used as an identification tool to ensure that cells isolated from tissue are in fact TM cells. It has also been shown that TM cells cultured on 2D plastic culture dishes have a lower expression of myocilin than native TM cells [43]. In this work, gene

expression was used to confirm the identity of TM cells isolated from porcine eye tissue. Two isolation procedures were performed over the course of this work, so both isolation products were tested. Quantitative real time PCR (qPCR) was used to determine the level of myocilin expression in TM cells treated with and without dexamethasone. A reference gene, GAPDH, was used to normalize the results using the  $\Delta\Delta C_t$  method. This method allows for comparison of relative levels of expression using both a reference gene and a calibrator [44]. For this method to be valid, the efficiency of amplification must be approximately the same for both the reference and target genes as the amount of cDNA is diluted. This ensures that the primers and probes used in the qPCR reaction are not affected by low cDNA concentrations. To test the efficiency, dilutions of cDNA are amplified for both the reference and target genes and the difference in threshold cycle ( $\Delta C_t$ ) between the two is plotted. A slope of less than 0.1 is considered evidence of an efficient reaction. **Figure 3.16** provides the efficiency plot for our qPCR reactions. MYOC was considered the target gene and GAPDH the reference gene. Figure 3.16 confirms that the  $\Delta\Delta C_t$  method can be used. A full derivation of the method can be found in the paper by Livak and Schmittgen [44]. The results, presented in **Figure 3.17**, show the relative levels of expression of myocilin in TM cells treated with and without dexamethasone. Figure 3.17 confirms that the samples treated with dexamethasone had a several fold increase in myocilin expression compared to controls that did not receive dexamethasone. This is the expected result for the inducible glucocorticoid response of TM cells. Future work will focus on the myocilin expression of TM cells cultured on collagen-GAG scaffolds.

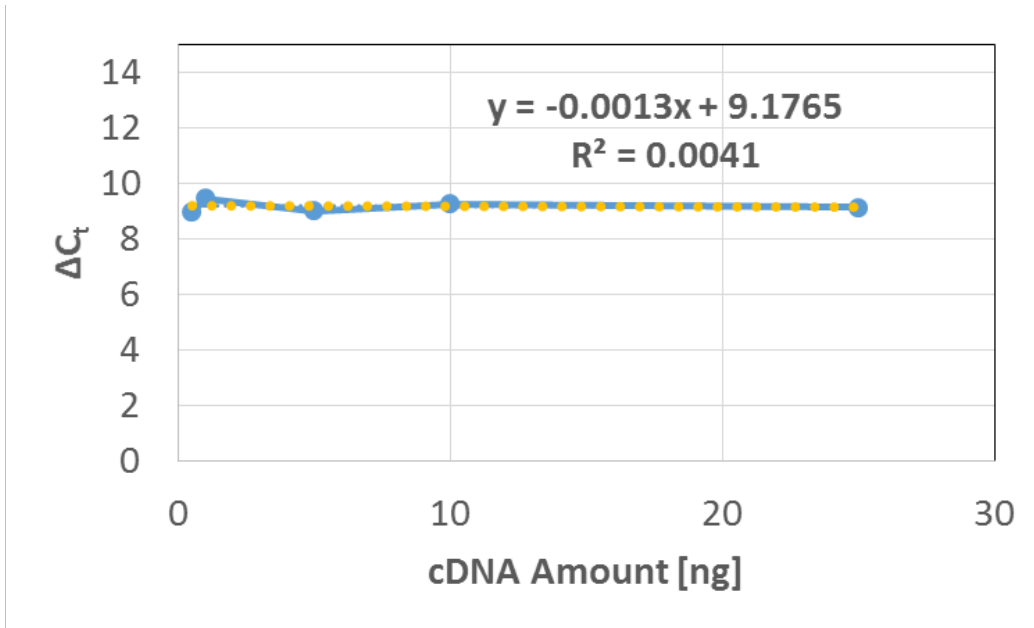


**Figure 3.16** - Efficiency plot for the qPCR reactions. The  $\Delta C_t$  represents the difference in threshold cycle between the target and reference genes ( $C_{t,MYOC} - C_{t,GAPDH}$ ). A cDNA dilution should result in very little change in the  $\Delta C_t$  values.

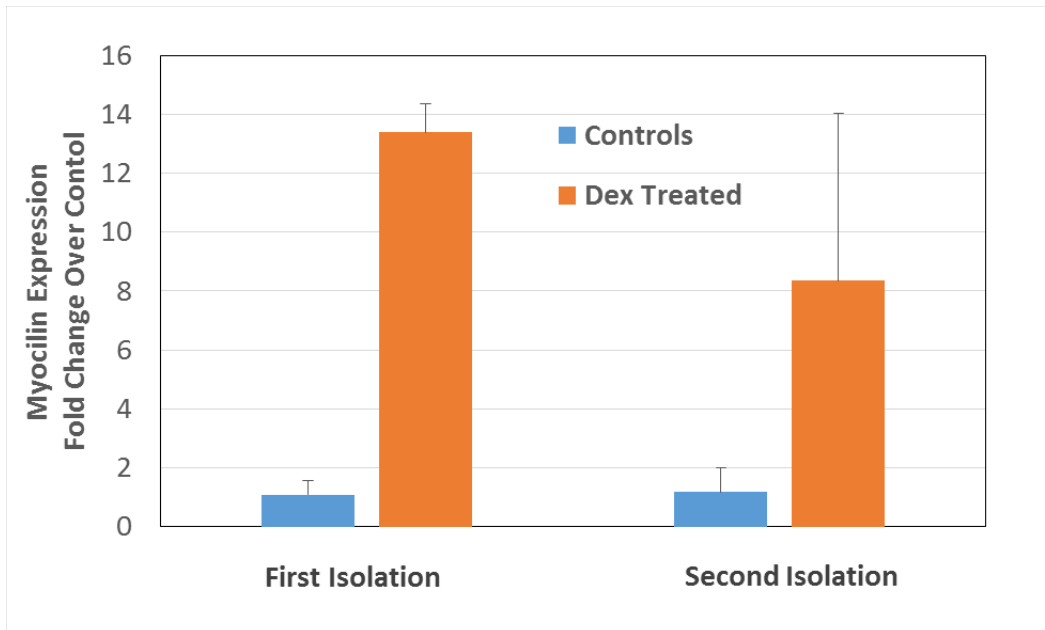


**Figure 3.17** - The fold change in expression of myocilin in TM cells treated with and without dexamethasone. Data are normalized against GAPDH reference genes and a control calibrator.

## CHAPTER 4

### SUMMARY AND RECOMMENDATIONS

#### 4.1 Summary of Results

The overall goal of this thesis work was to lay the groundwork for a 3-dimensional *in vitro* model of the trabecular meshwork. The blinding eye disease glaucoma is associated with elevated intraocular pressure due to insufficient outflow of aqueous humor through the trabecular meshwork. Because there is no cure for glaucoma, there is an abundance of research into therapeutics that can better treat the disease. Previous *in vitro* models have oversimplified the complex, 3D environment of the native TM. This work aimed to create a uniaxially aligned, porous, collagen-GAG scaffold to mimic the native TM and provide a platform for screening new glaucoma therapeutics.

Fabricated collagen-GAG scaffolds were characterized in a number of ways. Scanning electron microscopy was used to examine the internal and surface pore structure. Image analysis revealed that the average pore diameter of fabricated scaffolds was  $13.7 \pm 5.21 \mu\text{m}$  and the pore density was 2027 pores/mm<sup>2</sup>. These values were on the same order of magnitude as native TM [19-21]. Dynamic mechanical analysis was used to find the storage modulus of collagen-GAG and collagen-only scaffolds and it was found that they were statistically the same. Literature values, while not directly comparable, differed amongst each other. It was found that our storage modulus correlated well with an elastic modulus found by Russell *et al.* but was two orders of magnitude smaller than that found by Camras *et al.* [21, 23].

Glycosaminoglycan content was quantified using a DMMB assay. Two different crosslinking techniques, dehydrothermal crosslinking alone and dehydrothermal crosslinking plus EDC chemistry, were compared for the retention of GAG over time. There was no difference in retention over 2 weeks in solution. Over that time period, approximately 85% of the GAG was eluted. It was hypothesized that this is due to the saturation of available crosslinking sites between collagen and GAG [26-29].

TM cells cultured on collagen-GAG scaffolds were evaluated in terms of viability, proliferation, migration, and gene expression. Fluorescent stains were used to visualize TM cells on scaffolds from 3 days to 2 weeks after seeding. Images taken with confocal microscopy reveal that live TM cells with an elongated morphology could be seen over the course of this time period. An MTS assay was used to test the proliferation of TM cells on collagen-GAG scaffolds. The results show that TM cells proliferate quickly from 3 days to 1 week, and then begin to slow from 1-2 weeks. It was hypothesized that this decrease is due to the lack of cell-cell contact the TM cells experience as they begin to spread over the surface of the scaffold [17]. Histology was used to examine the migration and general location of TM cells on scaffolds. At low seeding densities, TM cells had limited migration into the internal structure and preferred to stay on the surface of the scaffolds. At higher densities, there was more migration inward. This behavior correlates well with the seeding technique used, called static seeding [36-38]. Finally, gene expression was employed to confirm the identity of TM cells by measuring the expression of the protein myocilin. Myocilin is expressed in higher amounts when TM cells are exposed to glucocorticoids [42, 43]. Results confirmed that the cells isolated from porcine tissue produced the expected response.

## 4.2 Recommendations for Future Work

This section contains my recommendations for improving the current state of the 3-dimensional *in vitro* model and provides an outline for the future directions of the project.

### 4.2.1 Increasing the Retention of Glycosaminoglycans

The current method of fabricating collagen-GAG scaffolds results in elution of most of the GAG over a 2 week time period in solution. While it was deemed to be acceptable for this phase of the project, it may be desirable in the future to increase this retention rate as GAGs play an important role in the filtering aspect of the TM and the resistance to outflow of aqueous humor [14]. Previous studies have shown that complete prevention of GAG elution cannot be achieved [27-29, 45]. There are methods that have slowed the elution rate, however. Choy *et al.* found that amination of collagen increased the retention of GAG when compared to untreated collagen [28]. Other chemical crosslinking techniques could also be employed to target different residues on both collagen and GAG. The concern with implementing these types of additional processing techniques is the introduction of chemicals that could result in cytotoxicity. Crosslinkers like glutaraldehyde have been shown to have detrimental effects on cell health [46]. Should GAG retention become an area of focus once more, extensive washing away of any chemical residues will need to be performed to ensure that cell health is not adversely affected.

#### 4.2.2 Scaffold Seeding Technique

Thevenot *et al.* showed that the distribution and migration of cells within a 3D construct is heavily influenced by the technique used deliver the cells to the construct [36]. Static seeding is widely used in tissue engineering due to its ease of use and high viability. Thevenot showed that static seeding results in minimal migration of cells into a 3D environment. In this work, histology revealed that with higher seeding densities, static seeding resulted in some migration into the internal structure, but the overall effectiveness of the model would be improved with more migration and penetration. Orbital seeding has been shown to distribute cells evenly throughout 3D constructs [36, 41, 47]. This method involves placing the scaffold and a cell suspension into a tube that cells cannot attach to and shaking with an orbital shaker for several hours. I believe that this method could have multiple benefits. First, a more even distribution of TM cells within the collagen-GAG scaffolds will better represent the native tissue and serve as a more realistic 3-dimensional *in vitro* model. Second, both the proliferation assay and histology provided evidence that too few TM cells results in retarded growth and migration due to lack of cell-cell contact. Using the orbital method, many more cells could be delivered to the scaffold taking into consideration the available surface area. With the static seeding method, the concentrated cell suspension becomes limited by the very small volume needed to deliver the cells only to the surface. Orbital seeding circumvents this problem by giving cells ample time to make their way into the pores of a 3D scaffold and distribute into the entire available area. My recommendation for future work would be to employ the orbital seeding method and repeat the proliferation assay

and histology analysis to determine whether this method alleviates the problems encountered.

#### **4.2.3 Myocilin Expression of TM Cells on Scaffolds**

Obtaining myocilin expression of TM cells seeded on collagen-GAG scaffolds could be another indicator that cells are behaving in a way similar to their native environment. It has been shown that TM cells cultured on 2D plastic have a lower expression of myocilin than native TM cells [43]. The expectation would be that TM cells cultured on collagen-GAG scaffolds would have a higher expression of myocilin than TM cells cultured on plates. Myocilin is thought to play an important role in the pathogenesis of glaucoma [48]. Mutant MYOC genes have been identified in glaucomatous tissues, sometimes leading to under expression of myocilin in the TM [49, 50]. Moving forward, myocilin expression may prove to be a source of valuable information regarding the effectiveness of potential glaucoma therapeutics. Current studies are underway to obtain the expression of myocilin in TM cells seeded on collagen-GAG scaffolds.

#### **4.2.4 Perfusion of Collagen-GAG Scaffolds**

The next chapter of this work will primarily focus on exposing this *in vitro* model to fluid flow. Trabecular meshwork tissue in the eye is constantly being perfused with aqueous humor. It is this flow that maintains the intraocular pressure. Normal eyes are typically maintained at approximately 15 mmHg with an average flow rate of 2.4  $\mu\text{L}/\text{min}$



[51]. Due to the aqueous outflow and fluctuations in intraocular pressure, TM tissue experiences biomechanical stresses such as fluid shear stress, mechanical stretching, and compression. During development and tissue maintenance, mechanical stress is a critical regulator of cellular behavior, altering the functional and structural properties of tissues [52]. TM cells are pressure-sensitive cells that experience mechanical stress throughout their lifetime [53, 54]. Furthermore, Johnson reported that *ex vivo* TM cells require a perfusion rate of at least 1  $\mu\text{L}/\text{min}$  for long-term survival [55]. Flow perfusion culture of cells seeded onto a 3-dimensional scaffold can both potentially provide fluid flow induced mechanical stimulation and permit true multilayered 3-dimensional cellular growth and organization. The next phase of this project will involve creating a perfusion system to mimic the flow of aqueous humor through the trabecular tissue. As a basis, a system similar in design to that used by Torrejon *et al.* will be used [13]. There will be control over the flow rate and the pressure will be approximated by measuring the back pressure of flow through the system. When a sufficient system is attained, known glaucoma therapeutics will be perfused and their effect on TM cells monitored. In theory, perfused glaucoma therapeutics should result in a decrease in the back pressure through the system. This will be the initial metric by which the drug efficacy is measured.

#### **4.3 Conclusion**

This thesis presents the development of a 3-dimensional *in vitro* model of the trabecular meshwork. Over the course of this work, three primary objectives were achieved. The first was to fabricate collagen and glycosaminoglycan tissue scaffolds

with uniaxially aligned pores. The second goal was to characterize these scaffolds with SEM, dynamic mechanical analysis, and glycosaminoglycan quantification. The third goal was to culture TM cells on fabricated scaffolds and explore their viability, proliferation, migration, and gene expression. Overall, this project laid the groundwork for an effective 3-dimensional *in vitro* model of the TM. Future work will focus on improving certain aspects of the current model as well as introducing perfusion to the system to mimic the flow of aqueous humor.

## REFERENCES CITED

- [1] G. Beidoe and S. Mousa, "Current primary open-angle glaucoma treatments and future directions," *Clinical Ophthalmology*, vol. 6, pp. 1699-1707, 2012.
- [2] National Eye Institute. (2010, January 8). *Glaucoma, Open-angle*.
- [3] R. Langer and J. Vacanti, "Tissue Engineering," *Science*, vol. 260, pp. 920-926, 1993.
- [4] U. Stock and J. Vacanti, "Tissue Engineering: Current State and Prospects," *Annual Reviews*, vol. 52, pp. 443-451, 2001.
- [5] M. Vert, Y. Doi, K.-H. Hellwich, M. Hess, P. Hodge, P. Kubisa, *et al.*, "Terminology for biorelated polymers and applications (IUPAC Recommendations 2012)," *Pure and Applied Chemistry*, vol. 84, pp. 377-408, 2012.
- [6] R. Bareil-Parenteau, R. Gauvin, and F. Berthod, "Collagen-Based Biomaterials for Tissue Engineering Applications," *Materials*, vol. 3, pp. 1863-1887, 2010.
- [7] M. Shoulders and R. Raines, "Collagen Structure and Stability," *Annual Review of Biochemistry* 78, 929-958, 2009.
- [8] E. Khor, "Methods for the treatment of collagenous tissues for bioprotheses," *Biomaterials*, vol. 18, pp. 95-105, 1997.
- [9] J. M. Gonzalez, Jr., S. Hamm-Alvarez, and J. C. H. Tan, "Analyzing Live Cellularity in the Human Trabecular Meshwork," *Investigative Ophthalmology & Visual Science*, vol. 54, pp. 1039-1047, Feb 2013.
- [10] E. R. Tamm, "The trabecular meshwork outflow pathways: Structural and functional aspects," *Experimental Eye Research*, vol. 88, pp. 648-655, Apr 2009.
- [11] J. A. Wood, C. T. McKee, S. M. Thomasy, M. E. Fischer, N. M. Shah, C. J. Murphy, *et al.*, "Substratum Compliance Regulates Human Trabecular Meshwork Cell Behaviors and Response to Latrunculin B," *Investigative Ophthalmology & Visual Science*, vol. 52, pp. 9298-9303, Dec 2011.
- [12] C. T. McKee, J. A. Wood, N. M. Shah, M. E. Fischer, C. M. Reilly, C. J. Murphy, *et al.*, "The effect of biophysical attributes of the ocular trabecular meshwork associated with glaucoma on the cell response to therapeutic agents," *Biomaterials*, vol. 32, pp. 2417-2423, Mar 2011.

- [13] K. Y. Torrejon, D. Pu, M. Bergkvist, J. Danias, S. T. Sharfstein, and Y. Xie, "Recreating a Human Trabecular Meshwork Outflow System on Microfabricated Porous Structures," *Biotechnology and Bioengineering*, vol. 110, pp. 3205-3218, Dec 2013.
- [14] P. A. Knepper, W. Goossens, M. Hvizd, and P. F. Palmberg, "Glycosaminoglycans of the human trabecular meshwork in primary open-angle glaucoma," *Investigative Ophthalmology & Visual Science*, vol. 37, pp. 1360-1367, Jun 1996.
- [15] S. R. Caliarì and B. A. C. Harley, "The effect of anisotropic collagen-GAG scaffolds and growth factor supplementation on tendon cell recruitment, alignment, and metabolic activity," *Biomaterials*, vol. 32, pp. 5330-5340, Aug 2011.
- [16] M. S. Ponticiello, R. M. Schinagl, S. Kadiyala, and F. P. Barry, "Gelatin-based resorbable sponge as a carrier matrix for human mesenchymal stem cells in cartilage regeneration therapy," *Journal of Biomedical Materials Research*, vol. 52, pp. 246-255, Nov 2000.
- [17] A. Llobet, X. Gasull, and A. Gual, "Understanding Trabecular Meshwork Physiology: A Key to the Control of Intraocular Pressure?," *American Physiological Society*, vol. 18, pp. 205-209, 2003.
- [18] Y.-G. Ko, N. Kawazoe, T. Tateishi, and G. Chen, "Preparation of Novel Collagen Sponges Using an Ice Particulate Template," *Journal of Bioactive and Compatible Polymers*, vol. 25, pp. 360-373, Jul 2010.
- [19] R. R. Allingham, A. W. Dekater, C. R. Ethier, P. J. Anderson, E. Hertzmark, and D. L. Epstein, "THE RELATIONSHIP BETWEEN PORE DENSITY AND OUTFLOW FACILITY IN HUMAN EYES," *Investigative Ophthalmology & Visual Science*, vol. 33, pp. 1661-1669, Apr 1992.
- [20] W. Trattler, P. Kaiser, and N. Friedman, *Review of Ophthalmology*, 2nd ed.: Elsevier, 2012.
- [21] P. Russell and M. Johnson, "Elastic Modulus Determination of Normal and Glaucomatous Human Trabecular Meshwork," *Investigative Ophthalmology & Visual Science*, vol. 53, pp. 117-117, Jan 2012.
- [22] L. J. Camras, W. D. Stamer, D. Epstein, P. Gonzalez, and F. Yuan, "Differential effects of trabecular meshwork stiffness on outflow facility in normal human and porcine eyes (vol 53, pg 5242, 2012)," *Investigative Ophthalmology & Visual Science*, vol. 55, pp. 2316-2316, Apr 2014.

- [23] L. J. Camras, W. D. Stamer, D. Epstein, P. Gonzalez, and F. Yuan, "Circumferential Tensile Stiffness of Glaucomatous Trabecular Meshwork," *Investigative Ophthalmology & Visual Science*, vol. 55, pp. 814-823, Feb 2014.
- [24] M. Haugh, M. Jaasma, and F. O'Brien, "The effect of dehydrothermal treatment on the mechanical and structural properties of collagen-GAG scaffolds," *Journal of Biomedical Materials Research Part A*, 2008.
- [25] K. Weadock, E. Miller, E. Keuffel, and M. Dunn, "Effect of physical crosslinking methods on collagen-fiber durability in proteolytic solutions," *Journal of Biomedical Materials Research*, vol. 32, pp. 221-226, 1996.
- [26] J. S. Pieper, A. Oosterhof, P. J. Dijkstra, J. H. Veerkamp, and T. H. van Kuppevelt, "Preparation and characterization of porous crosslinked collagenous matrices containing bioavailable chondroitin sulphate," *Biomaterials*, vol. 20, pp. 847-858, May 1999.
- [27] J. C. Salamone, *Polymeric Materials Encyclopedia: Regeneration Templates, Artificial Skin, and Nerves*, 1996.
- [28] A. T. H. Choy, K. W. Leong, and B. P. Chan, "Chemical modification of collagen improves glycosaminoglycan retention of their co-precipitates," *Acta Biomaterialia*, vol. 9, pp. 4661-4672, Jan 2013.
- [29] K. Shahin and P. M. Doran, "Strategies for Enhancing the Accumulation and Retention of Extracellular Matrix in Tissue-Engineered Cartilage Cultured in Bioreactors," *Plos One*, vol. 6, Aug 15 2011.
- [30] B. Yue, C. C. L. Lin, P. F. Fei, and M. O. M. Tso, "EFFECTS OF CHONDROITIN SULFATE ON METABOLISM OF TRABECULAR MESHWORK," *Experimental Eye Research*, vol. 38, pp. 35-44, 1984 1984.
- [31] M. B. Abelson, R. David, A. Shapiro, and J. McLaughlin, "Glaucoma Therapeutics 2013: A look at the safety and efficacy of various therapies for the disease, from pharmaceuticals to surgical implants," *Review of Ophthalmology*, vol. 13, 2013.
- [32] G. Sengbusch, C. Couwenbergs, J. Kuhner, and U. Muller, "Fluorogenic substrate turnover in single living cells," *Histochem J.*, vol. 8, pp. 341-350, 1976.
- [33] W. Hamel, P. Dazin, and M. A. Israel, "Adaptation of a simple flow cytometric assay to identify different stages during apoptosis," *Cytometry*, vol. 25, pp. 173-181, Oct 1 1996.

- [34] T. Mosmann, "Rapid colorimetric assay for cellular growth and survival: Application to proliferation and cytotoxicity assays " *Journal of Immunological Methods*, vol. 65, pp. 55-63, 1983.
- [35] J. A. Ramos-Vara and M. A. Miller, "When Tissue Antigens and Antibodies Get Along: Revisiting the Technical Aspects of Immunohistochemistry-The Red, Brown, and Blue Technique," *Veterinary Pathology*, vol. 51, pp. 42-87, Jan 2014.
- [36] P. Thevenot, A. Nair, J. Dey, J. Yang, and L. Tang, "Method to Analyze Three-Dimensional Cell Distribution and Infiltration in Degradable Scaffolds," *Tissue Engineering Part C-Methods*, vol. 14, pp. 319-331, Dec 2008.
- [37] Y. Q. Wan, Y. Wang, Z. M. Liu, X. Qu, B. X. Han, J. Z. Bei, *et al.*, "Adhesion and proliferation of OCT-1 osteoblast-like cells on micro- and nano-scale topography structured pply(L-lactide)," *Biomaterials*, vol. 26, pp. 4453-4459, Jul 2005.
- [38] C. S. N. Choong, D. W. Hutmacher, and J. T. Triffitt, "Co-culture of bone marrow fibroblasts and endothelial cells on modified polycaprolactone substrates for enhanced potentials in bone tissue engineering," *Tissue Engineering*, vol. 12, pp. 2521-2531, Sep 2006.
- [39] A. Nieponice, L. Soletti, J. Guan, B. M. Deasy, J. Huard, W. R. Wagner, *et al.*, "Development of a tissue-engineered vascular graft combining a biodegradable scaffold, muscle-derived stem cells and a rotational vacuum seeding technique," *Biomaterials*, vol. 29, pp. 825-833, Mar 2008.
- [40] Y. Li, T. Ma, D. A. Kniss, L. C. Lasky, and S. T. Yang, "Effects of filtration seeding on cell density, spatial distribution, and proliferation in nonwoven fibrous matrices," *Biotechnology Progress*, vol. 17, pp. 935-944, Sep-Oct 2001.
- [41] B. S. Kim, A. J. Putnam, T. J. Kulik, and D. J. Mooney, "Optimizing seeding and culture methods to engineer smooth muscle tissue on biodegradable polymer matrices," *Biotechnology and Bioengineering*, vol. 57, pp. 46-54, Jan 5 1998.
- [42] Z. T. Resch and M. P. Fautsch, "Glaucoma-associated myocilin: A better understanding but much more to learn," *Experimental Eye Research*, vol. 88, pp. 704-712, Apr 2009.
- [43] E. R. Tamm, P. Russell, D. L. Epstein, D. H. Johnson, and J. Piatigorsky, "Modulation of myocilin/TIGR expression in human trabecular meshwork," *Investigative Ophthalmology & Visual Science*, vol. 40, pp. 2577-2582, Oct 1999.
- [44] K. J. Livak and T. D. Schmittgen, "Analysis of Relative Gene Expression Data Using Real-Time Quantitative PCR and the  $2^{-\Delta\Delta C_T}$  Method," *Methods*, vol. 25, pp. 402-408, 2001.

- [45] I. V. Yannas, J. F. Burke, P. L. Gordon, C. Huang, and R. H. Rubenstein, "DESIGN OF AN ARTIFICIAL SKIN .2. CONTROL OF CHEMICAL-COMPOSITION," *Journal of Biomedical Materials Research*, vol. 14, pp. 107-132, 1980 1980.
- [46] V. Charulatha and A. Rajaram, "Influence of different crosslinking treatments on the physical properties of collagen membranes," *Biomaterials*, vol. 24, pp. 759-767, 2003.
- [47] D. J. Griffon, J. P. Abulencia, G. R. Ragetly, L. P. Fredericks, and S. Chaieb, "A comparative study of seeding techniques and three-dimensional matrices for mesenchymal cell attachment," *Journal of Tissue Engineering and Regenerative Medicine*, vol. 5, pp. 169-179, Mar 2011.
- [48] J. R. Polansky, D. J. Fauss, P. Chen, H. Chen, E. LutjenDrecoll, D. Johnson, *et al.*, "Cellular pharmacology and molecular biology of the trabecular meshwork inducible glucocorticoid response gene product," *Ophthalmologica*, vol. 211, pp. 126-139, May-Jun 1997.
- [49] Y. H. Liu and D. Vollrath, "Reversal of mutant myocilin non-secretion and cell killing: implications for glaucoma," *Human Molecular Genetics*, vol. 13, pp. 1193-1204, Jun 2004.
- [50] N. Jacobson, M. Andrews, A. R. Shepard, D. Nishimura, C. Searby, J. H. Fingert, *et al.*, "Non-secretion of mutant proteins of the glaucoma gene myocilin in cultured trabecular meshwork cells and in aqueous humor," *Human Molecular Genetics*, vol. 10, pp. 117-125, Jan 15 2001.
- [51] M. Goel, R. G. Picciani, R. K. Lee, and S. K. Bhattacharya, "Aqueous Humor Dynamics: A Review," *The Open Ophthalmology Journal*, vol. 4, pp. 52-59, 2010.
- [52] C.-P. Heisenberg and Y. Bellaiche, "Forces in Tissue Morphogenesis and Patterning," *Cell*, vol. 153, pp. 948-962, May 23 2013.
- [53] D. WuDunn, "Mechanobiology of trabecular meshwork cells," *Experimental Eye Research*, vol. 88, pp. 718-723, Apr 2009.
- [54] A. F. Clark, "The Cell and Molecular Biology of Glaucoma: Biomechanical Factors in Glaucoma," *Investigative Ophthalmology & Visual Science*, vol. 53, pp. 2473-2475, May 2012.
- [55] D. H. Johnson, "Human trabecular meshwork cell survival is dependent on perfusion rate," *Investigative Ophthalmology & Visual Science*, vol. 37, pp. 1204-1208, May 1996.